Ecological Indicators 154 (2023) 110854

Contents lists available at ScienceDirect

Ecological Indicators

journal homepage: www.elsevier.com/locate/ecolind

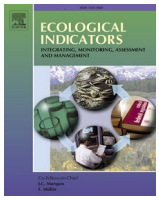

Original Articles

Using water sources extent during inundation as a reliable predictor for vegetation zonation in a natural wetland floodplain

Tomasz Berezowski [a,*], Martin Wassen [b]

[a] Faculty of Electronics, Telecommunications and Informatics, Gdansk University of Technology, Gabriela Narutowicza 11/12, 80-233 Gdansk, Poland
[b] Environmental Sciences, Copernicus Institute of Sustainable Development, Utrecht University, Princetonlaan 8a, 3584 CB Utrecht, The Netherlands

ARTICLE INFO

Keywords:
Wetlands
Inundation
Vegetation zonation
Water sources
Machine learning
Climate change

ABSTRACT

Distinctive zones of inundation water during floods were shown to originate from different sources in some major floodplains around the world. Recent research showed that the zonation of water in rivers and floodplains is related to vegetation patterns. In spite of this, water source zones were not used for vegetation modeling due to difficulties in their delineation. In this study, we used simulation results of a fully-coupled groundwater-surface water integrated hydrological model (IHM) HydroGeoSphere and the Hydraulic Mixing-Cell method to provide standard hydrological predictors (e.g. water depth, inundation length, groundwater depth, exchange flux) and the extent of inundation zones having a certain water source (discharged groundwater, river, rainfall, and snowmelt). These variables were used to train a vegetation model for the lower Biebrza floodplain (about 290 km^2) using vegetation maps from 1960, 1980, and 2000. We used a one-at-a-time (OAT) approach, where each map was validated based on a model trained on the remaining two maps to obtain realistic error estimates. We also used a fractional approach in which a fraction of each map was used for training and validation. The single model from the fractional approach was used to assess the importance of predictors and to predict vegetation for the 20th century and for the 21st century using IHM simulation forced by the Twentieth Century Reanalysis data and EURO-CORDEX RCP 2.6, 4.5, and 8.5 model ensembles. The model which used both water sources extent and standard predictors performed the best overall and was sensitive to the future trends. The extent of river water within the inundation area was by far the most important vegetation predictor. The models that neither used the water sources extent predictors nor the exchange flux were not able to predict the trends of areas covered by certain vegetation types under future climate. The advantage of the water sources extent predictors was their ability to represent the spatial effect of local hydrological phenomena. This was not possible with the standard predictors, because they show only the source of the phenomena (e.g. groundwater discharge zone), but do not indicate the actual area affected by its physical and chemical properties, which is more relevant for vegetation development. Our results highlight the relevance of using water extent predictors due to their ability to explain spatiotemporal ecological processes, such as vegetation development. We suggest to use water extent predictors in modelling for developing more accurate decision support for wetland floodplains.

1. Introduction

Flooding is considered to be the major driver affecting floodplain vegetation (Blom and Voesenek, 1996). Over the last decades basic surface water properties, such as surface water depths or inundation duration (Keddy, 1984; Ferreira and Stohlgren, 1999; Capon, 2005; Murray-Hudson et al., 2014), groundwater properties, such as depth of the groundwater table, or soil moisture content (Silvertown et al., 1999; Dwire et al., 2006; Jabłońska et al., 2011), and water chemistry indicators such, as electrical conductivity (EC) and pH (Ellery et al., 1993; Llampazo et al., 2022) were identified as relevant for floodplain vegetation development. Gradients in these chemical and physical properties can originate from water from different sources that can be present undiluted or be mixed with other water types. Due to extensive interactions between groundwater and surface water in wetlands, a considerable amount of research sources were invested in studying the relation between water chemistry and vegetation. An interesting phenomenon that facilitates suitable conditions for wetland vegetation is the mixing of groundwater with atmospheric water (precipitation, snowmelt) (Wassen and Joosten, 1996; Almendinger and Leete, 1998).

* Corresponding author.
E-mail address: tomberez@eti.pg.edu.pl (T. Berezowski).

https://doi.org/10.1016/j.ecolind.2023.110854
Received 27 February 2023; Received in revised form 16 August 2023; Accepted 19 August 2023
Available online 23 August 2023

The mixing process is, however, not only depending on local conditions, i.e., it does not occur only by on-site groundwater discharge or on-site high water tables but is a result of dynamic groundwater flow in the topsoil over wider areas which produces a spatial effect. This process of spatial interactions between groundwater flow and site conditions is of great relevance and was identified as a factor affecting the presence of fen species in different landscapes (Grootjans et al., 2006). The relevance of such spatial groundwater mixing was confirmed in a comparison study, which showed that the fen vegetation pattern was explained better by a model that used the zone of groundwater-affected soil as a predictor than a model that used only the groundwater discharge area i.e. the area where groundwater physically discharged (Van Loon et al., 2009). These studies showed that wetland vegetation can be modeled with various predictors that can discern the local or spatial effect of the hydrological system. However, the advantage of the latter predictors is that they provide a more realistic estimation of the area affected by properties of a water source (e.g. base-rich groundwater) that can result in a better vegetation model.

Mixing of water from different sources occurs not only below the ground surface but also and probably even more prominently in the inundation zone. Mixing of sediment-rich river water with sediment-poor water originating from floodplains or from tributaries was identified in several wetland floodplains of the world's largest rivers (Mertes, 1997). Yet the relationship between wetland vegetation and the zones of water from different sources in inundated conditions was investigated only in several studies. Identification of water zones conducted downstream of the confluence of the sediment-poor river Negro and the sediment-rich river Solimes-Amazon has shown that flooding of these two water types occurs on the opposite side of the floodplain (Park and Latrubesse, 2015) and corresponds to the presence of white-water and black-water vegetation types (Junk et al., 2012; Junk et al., 2015). Another study showed that the sediment concentration gradient occurring downstream the confluences of rivers in the Amazon catchment can define patterns of bird diversity by influencing floodplain productivity and forest structure (Laranjeiras et al., 2021). Except for the Amazon floodplain, several studies analyzed the relation between zones of water from different sources and vegetation in the Biebrza floodplain located in N-E Poland. The analysis of water sources extent in the Biebrza floodplain showed that the most productive vegetation (e.g. reed) is located in the river water zones, whereas in remote parts of the floodplain, where the continuous inundation was predominately formed by groundwater discharge and precipitation less productive fen vegetation (e.g. sedge-moss) was present (Chormański et al., 2011). Further analysis of this topic confirmed that the total extent of inundation is a poor predictor for the most productive vegetation, but also showed that the nutrient-rich sedimentation pattern is a better predictor for vegetation zonation than the river water extent (Keizer et al., 2018). In the scope of these studies, the spatial extent of water from different sources can be an important predictor for vegetation modeling, yet this research topic was not fully explored.

Hydrological predictors for floodplain vegetation models are usually obtained by interpolation (Peters et al., 2007; Todd et al., 2010; Anderson et al., 2023), hydrodynamic modelling (Mosner et al., 2015; Yao et al., 2020; Liang et al., 2020), or derived directly from point measurements (Ndehedehe et al., 2021; Peng et al., 2022). Alternatively, the integration of hydrodynamic and vegetation models can be used to simulate the water-vegetation interactions and to trace the development of vegetation over time. This approach has been applied by using CASIMIR (Benjankar et al., 2011) and other recently developed models (Zhu et al., 2020; Dang et al., 2022). In spite of being quite often applied, these approaches still do not or only very limited account for interactions between water sources, because they do not simulate water fluxes between the groundwater and surface water domains and do not trace the spatial extent of each water source. Effectively the influence of water from different sources on vegetation is not depicted by these approaches.

A solution for this issue is to use integrated hydrological models (IHM), which solve coupled 3D groundwater and 2D surface water flow (Sebben et al., 2013). Yet, IHMs are rarely used in ecological applications despite their advantages in solving complex problems, inter-domain interactions, and 2D/3D flow (Brewer et al., 2018). In a study aiming at the identification of riparian vulnerability an IHM was driven by historical meteorological data and the output was used to develop vegetation models, which were further used to predict future vegetation based on future climate scenarios (Fernandes et al., 2016). This appeared to be possible because IHMs are physically based and a model calibrated for the historical data should be valid also for future predictions. Another study used IHM output to model the distribution of meadow vegetation including endangered species (Gattringer et al., 2019). As shown in that study, vegetation modes performed significantly better when the IHM output was used for modeling in comparison to scenarios that used groundwater level observations, or interpolated river water level observations.

Although integrated hydrological models (IHMs) are useful in simulating interactions between sources of water and allow to simulate their collective hydrodynamic effect, they do not allow to quantitatively separate the effect of each water source spatially. To do this, one can use the Hydraulic Mixing-Cell (HMC) method (Partington et al., 2011), which allows to calculate and label time-varying fractions of each water source based on IHM simulated water fluxes. Application of HMC allowed to investigate streamflow generation mechanisms (Partington et al., 2013; Gutiérrez-Jurado et al., 2019), identify the sources of water in a riparian-stream continuum (Glaser et al., 2021), quantify groundwater and river water mixing in the groundwater domain (Nogueira et al., 2022), or delineate river-floodplain water zones (Berezowski et al., 2019). The latter study was conducted in the lower Biebrza floodplain to show that distinctive zones of water sources are present during flooding. These zones could serve as indicators of floodplain vegetation that, contrary to local predictors, would allow to investigate the spatial effect of water from different sources. Yet the HMC simulations of water zones were not used in vegetation modeling so far, nor was their suitability compared to local predictors such as surface water or groundwater levels.

In this study, we use simulation of water sources extents and other hydrological predictors for floodplain vegetation modelling. We will set up a vegetation model for the Biebrza River floodplain, where relations between vegetation and water sources extent during inundation were documented before and which, due to its well-studied use as a reference area for other river floodplains, allows to transfer the results to similar wetland floodplains. Our aim is to test several sets of model predictors that reflect the most common modelling practice with using only standard, local groundwater, and surface water predictors, with a less common practice, i.e. more complex interactions between groundwater and surface water by use of a novel approach based on water source extent predictors. We hypothesize that predictors based on the simulated extent of certain water sources increase the accuracy of the floodplain vegetation model in comparison to predictors based on standard groundwater and surface water variables. The results of this study may demonstrate the relevance of using hydrological predictors that depict the spatial effect of a water source on wetland vegetation types. To assure reliable validation of our hypothesis we test the vegetation models using three vegetation maps (from 1960, 1980, and 2000). The deep investigation of each model behavior is investigated by analysis of the difference in prediction under the past (since 1900) and future (till 2099; three greenhouse gas emission scenarios) hydrological and climatic conditions.

2. Methods

Below we present the outline of the methods used in this study:

1. The integrated hydrological model (Section 2.3) for groundwater and surface water simulated water levels, water fluxes, and fractions of river, groundwater, snowmelt, and rainfall water in the Biebrza River catchment (Section 2.1) for the 1881–2099 period.
   a. The future simulations (2006–2099) were conducted using an ensemble of models for three greenhouse gas emission scenarios.
2. A subset of the hydrological model output was selected for the nodes in the floodplain area and aggregated to yearly values (Table 1) to develop the predictors for the vegetation model.
3. Floodplain vegetation maps from 1960, 1980, and 2000 were generalized to present the same vegetation types, which are used as a response variable in the vegetation model (Section 2.2).
4. A random forest model was trained to predict vegetation type based on hydrological predictors in each hydrological model node with a valid vegetation type (Section 2.4).
   b. Four scenarios were used to identify the optimal hydrological predictors for floodplain vegetation modelling.
   c. Final vegetation type prediction in a given year was obtained by majority voting from predictions in eight preceding years and the given year.
   d. A fraction of data from all three maps was used to train the model for the prediction of vegetation change in the 1910–2099 period. For the future period, vegetation prediction was conducted for each ensemble member.
   e. A one-at-a-time procedure was used for a fair assessment of the vegetation model accuracy for each map.

Table 1
Predictors calculated based on daily simulations in each node of the IHM for each year in the 1900–2000 period using the 20CR forcing data and in the 2006–2099 period using the RCP 2.6, 4.5, and 8.5 EURO-CORDEX forcing data ensembles.

Predictor	Symbol	Description	Group
Yearly mean of daily surface water depth	h_{sw}	Daily surface water depth (h) is an output of the IHM.	surface water
Number of days with water depth > 1 cm per year	l_1	Sum of days with h > 1 cm in a given year.	surface water
Number of days with water depth > 10 cm per year	l_{10}	Sum of days with h > 10 cm in a given year.	surface water
Yearly mean depth to groundwater table	h_{gw}	Daily groundwater head (output of the IHM) in the top layer subtracted from the surface elevation.	groundwater
Yearly mean soil saturation	m	Daily soil saturation in the top layer is an output of the IHM.	interactions
Yearly mean exchange flux	e	Mean daily exchange flux (e_0) between groundwater and surface water. e_0 is an output of the IHM.	interactions
Yearly mean surface water infiltration	e_i	Mean e_0 only if $e_0 < 0$	interactions
Yearly mean groundwater discharge	e_d	Mean e_0 only if $e_0 > 0$	interactions
Yearly mean rainfall fractions	f_{rain}	Fractions of water sources represent the volume fraction of each water source in the IHM node contributing area and are an output of the HMC module (Partington et al., 2011).	mixing
Yearly ean snowmelt water fractions	f_{snow}		mixing
Yearly mean groundwater fractions	$f_{groundwater}$		mixing
Yearly mean river water fractions	f_{river}		mixing
Yearly mean mixing degree	d	Dimensionless mixing degree between the river and floodplain water Berezowski et al. (2019), calculated as $d = 1-(\lvert f_{river}-f_{floodplain}\rvert/(1-f_{initial}))$, where $f_{floodplain} = f_{rain} + f_{snow} + f_{groundwater}$, and $f_{initial}$ is a very small fraction of water from initial conditions. The d values range between 0 and 1 and d = 1 indicates 1:1 mixing between floodplain and river water, whereas d = 0 indicates that only one water source is present in the model node.	mixing

2.1. Study area

The Biebrza catchment, located in north-eastern Poland, comprises 7091 km^2 (Fig. 1). The lower Biebrza valley (about 290 km^2), where we perform the vegetation modeling, is located along the river section downstream of the town Osowiec and upstream of the confluence with the Narew River. For several reasons, we choose the lower Biebrza valley (hereinafter referred to as floodplain) for vegetation modelling. First, the relationship between vegetation and hydrology was documented in the floodplain for a long period of time (Pałczyński, 1984). Next, the floodplain is considered a reference site for similar wetlands in the temperate zone where river floodplain and fen vegetation show near-natural patterns (Wassen et al., 2006). Finally, the floodplain as well as the catchment were not subjected to major river regulation works. The melioration of the floodplain was finished in the middle of the 19th century, whereas the major interference into the Biebrza River, which was the construction of a waterway to the Neman River, was finished in the first half of the 19th century (Banaszuk, 2004). Also, the human influence is rather low because currently, the Biebrza catchment is the least populated region in Poland (Statistics Poland, 2021), population density is expected to decline in the 21st century (Eurostat, 2019) and the Biebrza National Park is protected. Therefore, the study area is suitable for naturally driven vegetation development modeling over the 19th-21st centuries period and the results of this study are to some extent transferable to similar temperate zone wetlands elsewhere.

Vegetation in the floodplain has a predominantly lateral zonation perpendicular to the river. Nearest to the river narrow patches of compact willow (Salix) bushes and tall grass vegetation (Phalaridetum arundinaceae, cf Pałczyński, 1984) are present. Next, up to about 900 m from the river reed vegetation belonging to Phragmitetum communis and Glycerietum maximae can be observed. Further away, up to about 2500 m from the river, tall sedge vegetation belonging to Caricetum elatae and Caricetum gracilis are present. Finally, up to the upland margin fen vegetation, consisting of short growing sedges, forbs and mosses referred to as sedge-moss vegetation (e.g. Carici-Agrostietum caninae, Caricetum appropinquata, Caricetum diandrae) is present. The floodplain contains several dunes, which are mostly covered with forest. Alder and birch forests are also located close to the upland margin, around the dunes, and in a large complex in the southern part of the floodplain. The Biebrza floodplain was used for grazing and mowing in the last centuries, but the intensity of this management decreased in the end of the 20th century. Since the establishment of the Biebrza National Park grazing and mowing have been continued as a conservation practice (Kotowski et al., 2013; Berezowski et al., 2018).

The floodplain soils consist in the majority of various types of peat (Gnatowski et al., 2010) with depths up to 3 m, which were formed on top of the Quaternary sands and tills (Banaszuk, 2004). Near the river, fluvio-soils were formed consisting of alluvial deposits in a 300–1500 m belt. The upland around the floodplain consists of sands and glacial tills deposited during the Riss glaciation (Banaszuk, 2004).

The climate is humid continental according to the Köppen classification with a yearly precipitation (1970–2005) of 672 mm (88 mm snowfall), and a yearly potential evapotranspiration of 621 mm (IMGW-

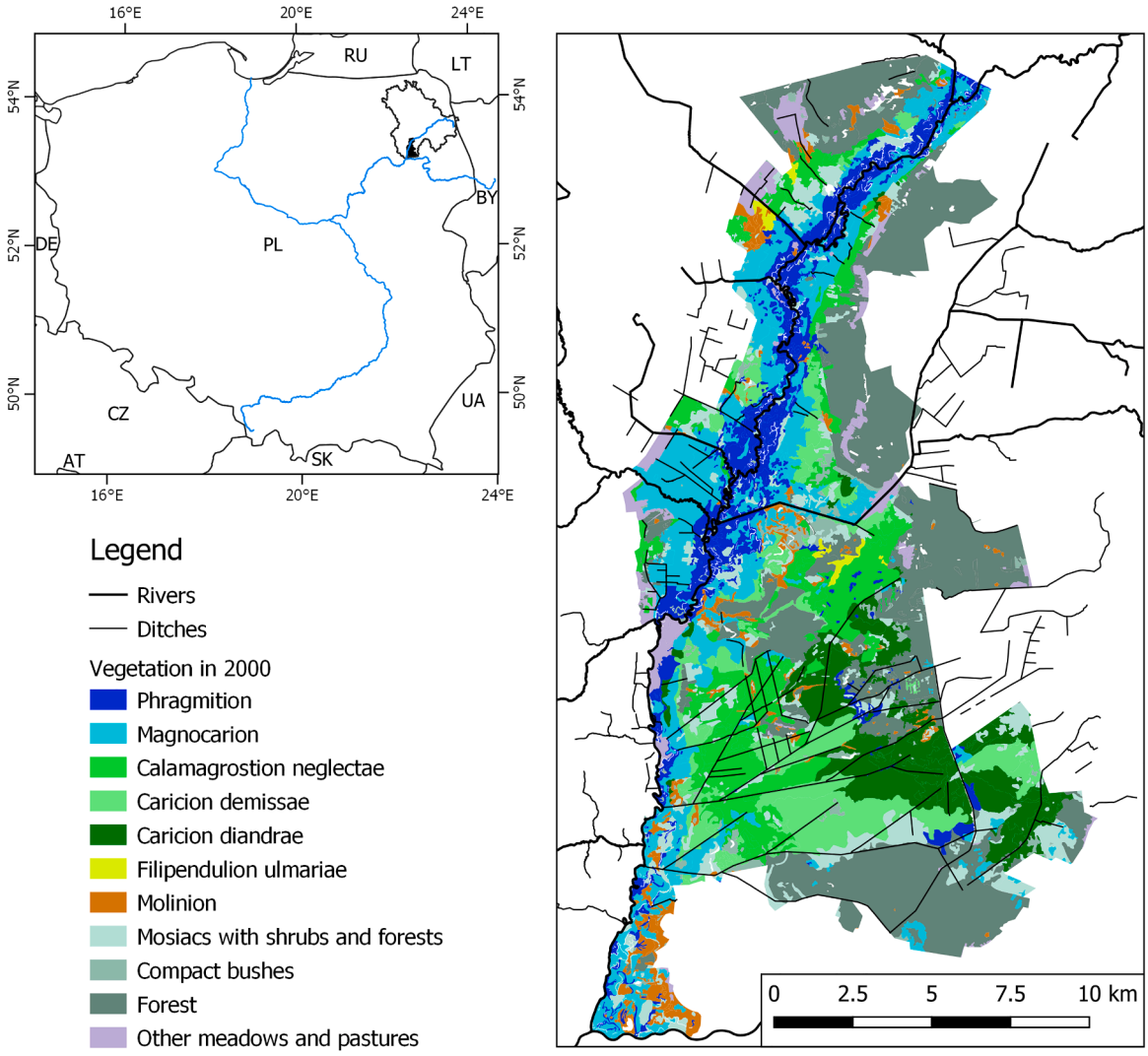

Fig. 1. Lower Biebrza valley floodplain with the river network and vegetation in 2000 (Matuszkiewicz et al., 2000) (right panel). Location of the Biebrza catchment study area (black outline) and the floodplain (black patch) in Poland (left panel); the major rivers Wisla, Bug, Narew and Biebrza are indicated with blue lines. The legend concerns only the right panel. (For interpretation of the references to color in this figure legend, the reader is referred to the web version of this article.)

PIB, 2019; JRC, 2019). The long-term yearly runoff (1970–2005) of Biebrza River is 169 mm, which corresponds to a mean daily discharge of 38.1 m^3s^{-1} (IMGW-PIB, 2019).

2.2. Vegetation maps processing

We used three vegetation maps, which were developed by field surveys and represent actual vegetation in the floodplain around 1960 (Oświt, 1968), 1980 (Pałczyński, 1984), and 2000 (Matuszkiewicz et al., 2000) (Fig. 2). Each map was developed by different authors and had methodological differences. We expect that the older maps might be characterized by lower accuracies, due to lower resources available at that time. Moreover, each map has slightly different vegetation types. To minimize the effect of the methodological differences between the maps and to reduce the uncertainty related to the older maps we performed generalization of the vegetation maps into generic wetlands vegetation types: Phragmition (reeds), Magnocaricion (tall sedges), sedge-moss, and other. All vegetation that could be unambiguously classified as Magnocaricion, Phragmition, or sedge-moss were merged respectively. Small vegetation patches that were not possible to resolve, but were within or adjacent to identifiable patches were merged accordingly. The other vegetation type consisted in majority of forests, however, it also included open water, non-wetland vegetation (present on sand dunes), and anthropogenic vegetation that could not be resolved. The exact merging approach for each map is presented in Table S1-S4.

2.3. Hydrological model

We used the HydroGeoSphere (Beumer et al., 2007; Hwang et al., 2014) IHM for the simulation of 2D surface water flow and 3D groundwater flow in the 7091 km^2 Biebrza catchment (Fig. 1 left panel). The model was chosen due to its robustness illustrated by previous ecohydrological applications (e.g. Werner et al., 2021; Nogueira et al., 2021; Houzé et al., 2022) and its ability to simulate the water source fractions of inundation water. The fraction of river flooding, groundwater discharge, snowmelt, and rainfall water volume in each model node was calculated based on the IHM output using the HMC method (Partington et al., 2011), which can be included in the HydroGeoSphere IHM. The model was forced using the Twentieth Century Reanalysis (20CR) data (Slivinski et al., 2019) for the period 1881–2015 and using an ensemble of ten EURO-CORDEX (Jacob et al., 2014) simulations for representative concentration pathways (RCP) 2.6, 4.5, and 8.5 for the 2006–2099 period (Table S5; only five-member ensemble in RCP 2.6). The detailed model description and validation are presented in Berezowski and Partington (2023), whereas the simulation output along with the vegetation maps used in this study are accessible in a repository

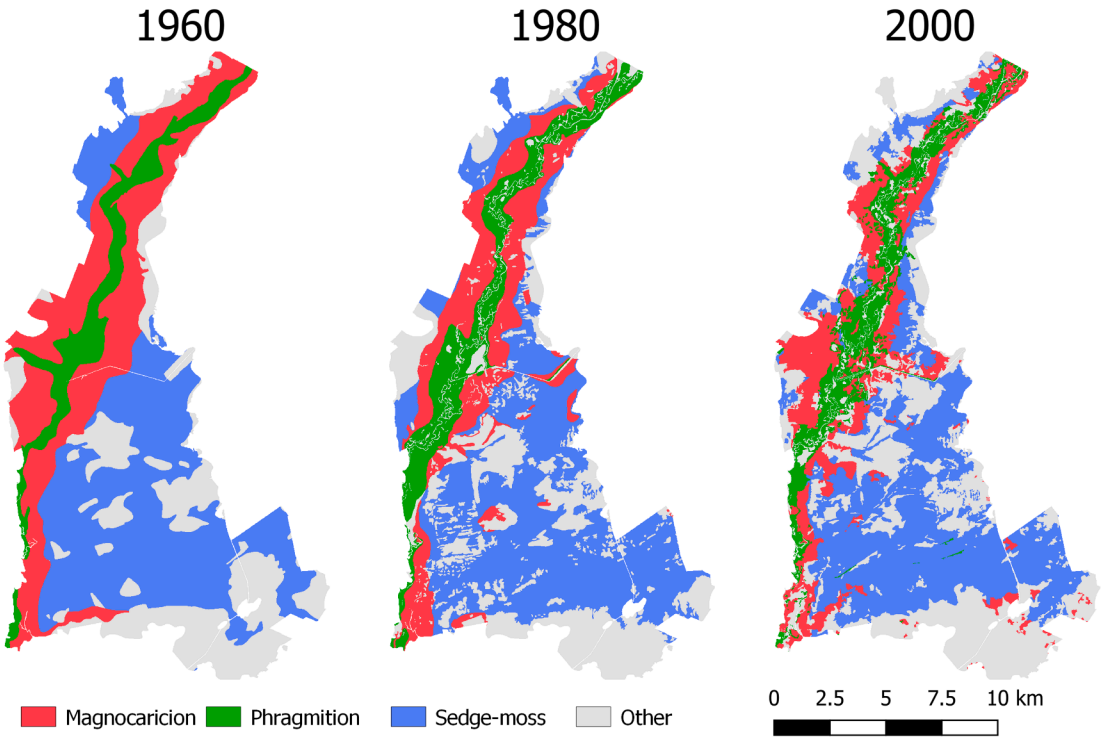

Fig. 2. Comparison of the vegetation maps used in this study after generalization into four types.

(Berezowski, 2023). The water levels error magnitude in two stations in the floodplain estimated by the root mean square error (RMSE) were low: 0.37 m, which corresponds to 9% and 10% of the data range for Burzyn gauge station (1930–2017 with gaps) and Osowiec gauge station (1881–2017 with gaps) respectively. Nine groundwater wells level in the floodplain area had also a low average RMSE of 0.28 m or 23% of the data range in the 1998–2019 period (with gaps). The low errors mean that the IHM was capable to simulate the hydrodynamics of the study area properly. Therefore the predictors derived from the IHM output can be used for explaining hydrology-related phenomena in the study area. In the surface layer, the model consisted of 19,297 nodes and 38,081 triangular elements of which 10,436 were in the floodplain, hence the median element size in the floodplain was 20037 m^2 and the minimum element area was 1017 m^2.

In a former study, the IHM simulations using HMC were analyzed in the scope of the length of the period in which a given water source was dominant in a model node, i.e., whether it persists longer or shorter in the inundation (Berezowski and Partington, 2023). In the 1881–1949 period a stable composition of river flooding, groundwater discharge, snowmelt, and rainfall water was present in the inundation. In the 1950–2015 period, which includes the years for which vegetation maps were used, several local trends were observed in the composition of water sources and in the period of surface water levels greater than 1 cm. In the 1950–2015 period, the water sources' composition, inundation period and mean water depth showed very clear changes in simulation for the future climate RCP scenarios.

We extracted the IHM output for the 290 km^2 floodplain area (Fig. 1 right panel) and aggregated the daily temporal resolution to a yearly scale to extract predictors for vegetation modeling in each IHM node (Table 1). The surface water domain properties, such as HMC output, exchange flux, and water depth were calculated directly from the surface water nodes. The groundwater properties, such as soil saturation and groundwater head were calculated for the top layer of the groundwater domain model grid. The spatially averaged predictors in the floodplain area for the 1900–2015 period are presented in Figure S1.

2.4. Vegetation modeling

We used the random forest classifier to model the vegetation type (Phragmition, Magnocaricion, or sedge-moss) using the IHM predictors (Table 1). The random forest algorithm was selected due to its ability to handle noisy predictors, parameter importance estimation feature, and resistance to overfitting (Breiman, 2001; Fox et al., 2017). Random forest was used in recent studies concerning floodplain vegetation modelling (Jing et al., 2023; Illeperuma et al., 2023). In this algorithm, a subset of predictors and samples are chosen randomly to form splits in each tree. The final predictor (vegetation type) is determined by majority voting over all trees in the forest. The number of trees (ntree) and the number of predictors sampled on each split (mtry) are the random forest *meta*-parameters. The ntree was 500 and the maximum mtry was 10 in this study.

The response variable (vegetation type) of the random forest model was aggregated for each IHM node to match the spatial representation of the predictors. The aggregation was realized by selecting the major vegetation type in the node contributing area. If no vegetation type covered more than 50% of the node contributing area then the node was excluded from the data set.

To test the hypothesis that predictors based on simulated water sources' extents increase the accuracy of the floodplain vegetation model, we used the following scenarios of the predictors set based on the groups indicated in Table 1:

1. only predictors from the "surface water" group, hereinafter referred to as SW,
2. predictors from "surface water" and "groundwater" groups, hereinafter referred to as GW-SW,
3. predictors from "surface water", "groundwater", and "interactions" groups, hereinafter referred to as GW-SW interactions,
4. only predictors from the "mixing" group hereinafter referred to as Mixing,
5. predictors from all groups, hereinafter referred to as Full.

We used two approaches for training and validation. The first approach was used to test the skill of the model for the prediction of vegetation in a period that was not present in the training set. In this approach, we used random 150 samples per vegetation type from two out of three vegetation maps to train the model (i.e. 300 samples per vegetation type in total). The prediction and validation were done on all samples from the third vegetation map, that is 3620 for the 1960 map, 3351 for the 1980 map, and 3069 for the 2000 map. Since the training and validation process was repeated three times - once for each vegetation map, hereinafter we name this approach one-at-a-time (OAT). The OAT approach provides more realistic accuracy estimates for the prediction of data not used for training. Yet, three models are developed in this approach, which is unsuitable for prediction in real-life applications. The second approach was used to train and validate a single prediction model based on all available vegetation maps. In this approach, we used random 150 samples per vegetation type for all three maps to train the model (i.e. 450 samples per vegetation type in total). The validation was done for the samples not used for training in each vegetation map, that is 2079 for Magnocaricion, 2533 for Phragmition, and 3579 for sedge-moss. We name this approach hereinafter fractional. The model obtained from the fractional approach was used to predict the vegetation types for the IHM predictors in the historical and future periods 1900–2099.

The predictors were calculated for a yearly period. We, however, expected that vegetation is an effect of hydrological processes over a longer period. Therefore both in OAT and fractional approaches we use two-level vegetation modeling. On the first level, we predicted the vegetation in a year x based on hydrological predictors from each year between x and x-n. In the second level, we choose the final predicted vegetation for the year x by majority voting out of all predictions in the period x to x-n years. In a preliminary study, we estimated experimentally that the best $n = 8$ in our case, i.e., in total each model uses 9 years of data. For $n = 8$ the accuracy of our models was greater than for $n < 8$, while for n greater than 8 accuracy did not increase considerably.

The overall model performance was evaluated using overall accuracy [%]:

$$\mathrm{acc} = 100 * y_p/y \quad (1)$$

where y_p is the number of IHM nodes with correctly predicted vegetation type and y is the total number of nodes used for validation. We calculated the confidence interval for the accuracy using the exact binomial test (Hollander et al., 2015). We assumed that the accuracy distribution could be approximated by the normal distribution and used a two-tailed Z-test with the $p = 0.05$, to check if the accuracies are significantly different one from another. We evaluated the model performance for each vegetation type using the F1 score [-], which is a harmonic mean of precision and recall [-]:

$$\mathrm{F1} = 2(\mathrm{precision} * \mathrm{recall}) / (\mathrm{precision} + \mathrm{recall}) \quad (2)$$

where precision is a ratio of true positive predictions to all predictions in a given vegetation type and recall is a ratio of true positive predictions to all validation samples of a given vegetation type observed in the map. The maximum value is F1 = 1 and in this case, the predicted and observed vegetation samples match exactly. The lower the precision or recall the lower the F1 and the minimum value of F1 = 0 is obtained when precision or recall is 0. The F1 score is calculated for individual samples (i.e. IHM nodes with a vegetation type label) and does not take into account uneven node area. Therefore, to quantify the misclassified area in each vegetation type we calculated the difference in the predicted and observed vegetation type for each map.

We tested the importance of the predictors for the models using the permutation importance in the fractional approach, which provided a single model per scenario. The permutation importance compares the performance of a model with the original values of a predictor with a model with randomly permuted values of the predictor. If the performance of both models is similar the predictor is not important. If the model with permuted predictor performed worse than the predictor is important. We choose to quantify the model's performance in the permutation importance experiment using the mean decrease of accuracy, which calculates the difference between accuracy in the original and permuted predictor model and averages over all trees in the random forest. We estimated the importance of the entire model and each vegetation type predicted in the model. The permutation importance used the models from the fractional approach, which provided a single model per scenario.

3. Results

3.1. Modelling scenarios validation

The overall accuracy of the models in the OAT approach was the highest for each map in the Full scenario (Fig. 3) with a mean of 82%. The Mixing scenario performed similarly (mean accuracy was 81%) to the Full scenario with the accuracy of the Mixing scenario not being significantly different between these two scenarios for each map. The GW-SW interactions scenario had lower accuracy (mean of 79%) than the Mixing scenario and the difference was significant except for the 2000 map. The SW and GW-SW scenarios performed similarly one to another (not significantly different) with the lowest accuracy in all maps (the mean was 74% in each scenario). In all scenarios, accuracy decreased with the increasing year of vegetation maps development (from 1960 through 1980 to 2000) and the accuracy was significantly different between the 1960 and 2000 maps.

In the fractional approach, the accuracy was higher (except for the 1960 and 1980 maps in the GW-SW interactions) for the corresponding cases in the OAT approach but the differences were not significant except for the 2000 map in the Mixing scenario (Fig. 3). The mean accuracy was 74% for SW, 75% for GW-SW, 78% for GW-SW interactions, 83% for Mixing, and 83% for Full scenarios. The accuracy pattern was similar to that in the OAT approach except that the Mixing scenario had higher accuracies than the Full scenario for 1960 and 2000 maps (not significantly different), and the GW-SW interactions scenario accuracy was significantly different from the Mixing scenario accuracy for the 2000 map. As in the OAT approach, the accuracy decreased with the increasing year of vegetation maps development but the difference between the 1960 and 2000 maps was significant only for SW, Mixing, and Full scenarios.

The F1 score in the OAT approach was highest for the sedge-moss and lowest for the Magnocaricion vegetation type (Fig. 4). The Mixing and Full scenarios performed similarly in each vegetation map with the highest F1 score for all vegetation types. The SW, GW-SW, and GW-SW interaction scenarios had similar F1 scores for the Magnocaricion in both approaches. The GW-SW interaction had higher F1 for Sedge-moss and Phragmition than SW and GW-SW scenarios in the OAT approach. The Magnocaricion vegetation type was the only one that decreased over time (1960–2000; Fig. 4). A similar pattern of F1 score as in OAT was observed for the fractional approach. The differences between corresponding scenarios and vegetation types from Fractional and OAT approaches were smaller than 0.01 except for the Magnocaricion and Phragmition vegetation in the SW scenario (-0.017 and 0.021 difference respectively), Phragmition vegetation in the GW-SW scenario (0.024 difference), and Magnocaricion and Phragmition vegetation in the Mixing scenario (-0.021 and 0.030 difference respectively).

The temporal change of vegetation types in the three maps was well reflected by the vegetation models both in fractional and OAT approaches (Fig. 5) The exception was the Phragmition for the 1960 and 1980 maps, where all models predicted the opposite trend of vegetation change than observed. Both in the OAT and fractional approaches the biggest difference in the area was observed for the Phragmition vegetation type and the lowest for Sedge-moss (Table 2). The mean absolute differences between the predicted and observed vegetation were 6.4%

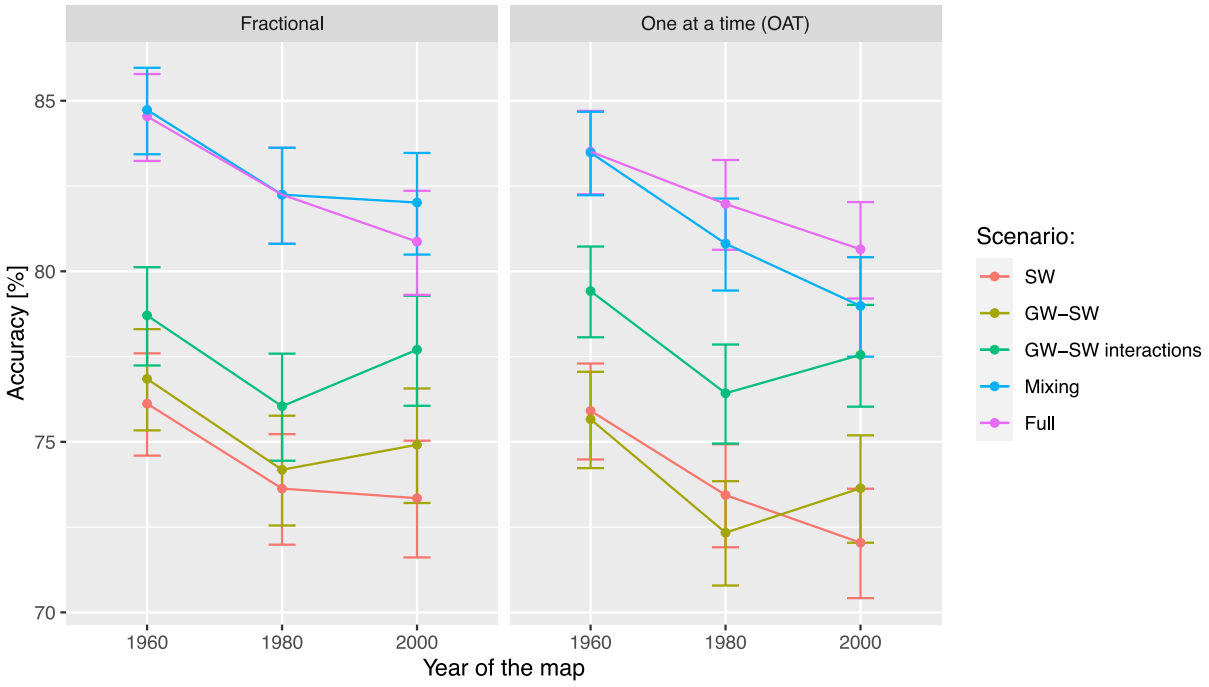

Fig. 3. Overall accuracy and the 95% confidence interval from the fractional (left) and OAT (right) validation approach for the five scenarios and three vegetation maps.

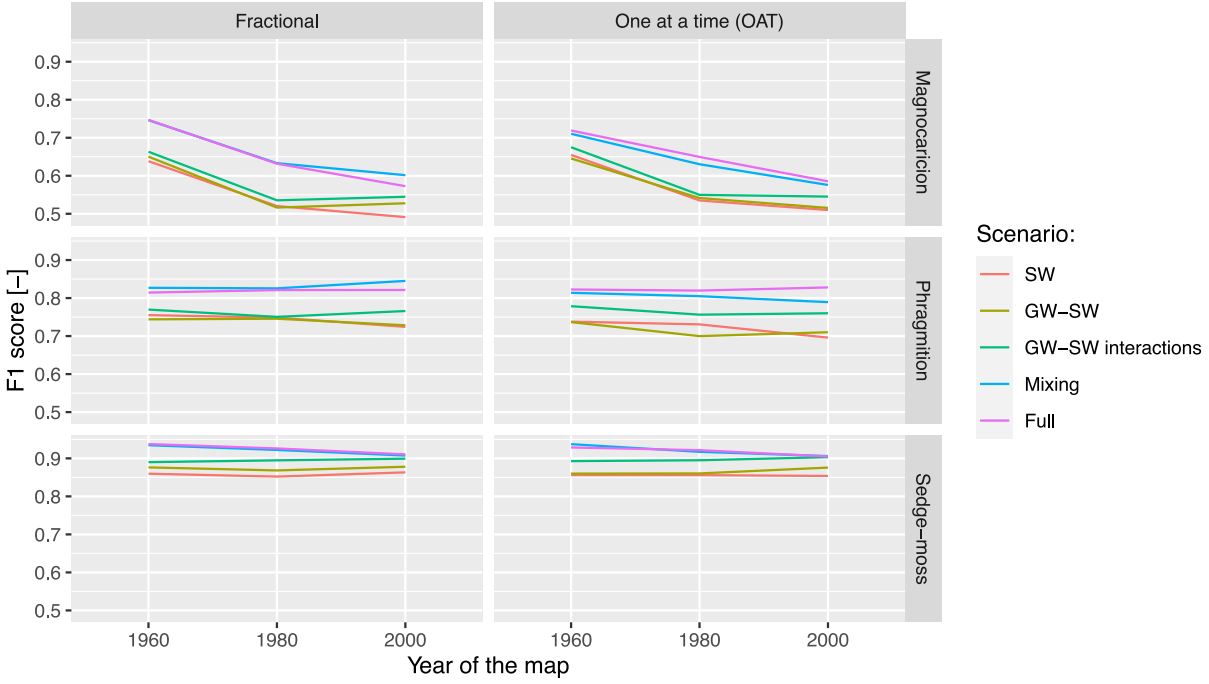

Fig. 4. The F1 score from the fractional (left) and OAT (right) validation approach for the five scenarios, three vegetation maps, and three vegetation types.

for SW, 7.3% for GW-SW interactions, 10.0% for Full, 10.1% for GW-SW, and 11.9 for Mixing scenarios in the OAT approach, and 9.5% for Full, 10.5% for GW-SW, 10.9% for Mixing, 11.5% for SW, and 12.2% for GW-SW interactions scenarios in the fractional approach.

3.2. Predictors importance

The highest importance in the Full scenario was observed for the mean river water fractions, f_{river}, with the next most important predictors also belonging to the "mixing" group: f_{snow}, and f_{rain} (Fig. 6). The most important predictors in the Full scenario which did not belong to the "mixing" group were related to the exchange flux between groundwater and surface water (e_d and e). Scenarios, which did not use predictors from the "mixing" group had the highest importance for the number of days with water depth greater than 10 cm (l_{10}) in SW and GW-SW, and e in GW-SW interactions. The SW and SW-GW scenarios had a similar pattern of the predictors' importance except for mean surface water depth (h_{sw}). The mean mixing degree predictor (d), used in the Full and Mixing scenarios, had moderately low importance in comparison to other predictors.

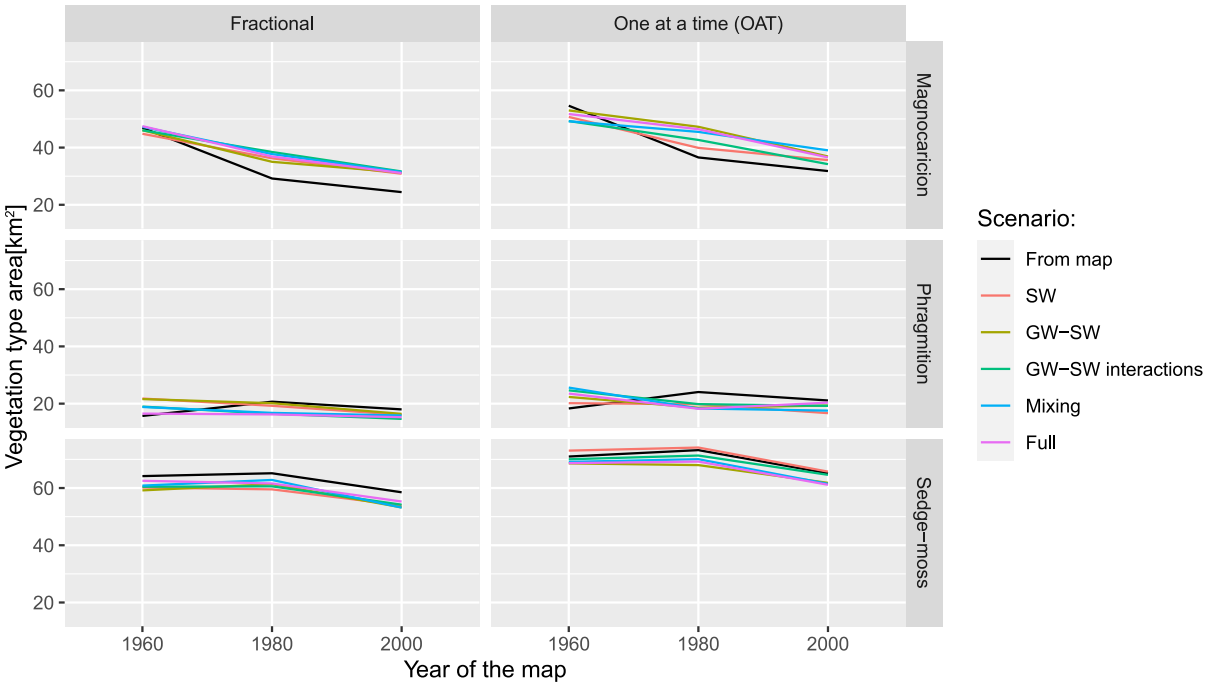

Fig. 5. Predicted and observed (from the map) areas of vegetation types in the fractional (left) and OAT (right) validation approach for the five scenarios, three vegetation maps, and three vegetation types. Areas of vegetation types are smaller in the fractional than in the OAT approach, because in the fractional approach, validation was made only on the validation sub-sample in each map.

Table 2
The absolute difference in area between predicted and observed vegetation type averaged from three maps (1960, 1980, and 2000) in the fractional and OAT approaches. Values in brackets show the difference as a percentage of the observed vegetation type area. Areas of vegetation types are smaller in the fractional than in the OAT approach, because in the fractional approach, validation was made only on the validation sub-sample in each map.

Vegetation type	Scenario	Predicted vegetation area absolute difference [km^2]	
		Fractional	One at a time (OAT)
Magnocaricion	SW	5.2 (15%)	3.7 (9%)
	GW-SW	4.5 (13%)	5.8 (14%)
	GW-SW interactions	5.8 (17%)	4.6 (11%)
	Mixing	5.3 (16%)	7.2 (18%)
	Full	5 (15%)	5.8 (14%)
Phragmition	SW	3.1 (17%)	3.5 (17%)
	GW-SW	2.7 (15%)	3.8 (18%)
	GW-SW interactions	3.6 (20%)	4.1 (20%)
	Mixing	3.1 (17%)	5.5 (26%)
	Full	2.7 (15%)	3.9 (19%)
Sedge-moss	SW	4.7 (8%)	1.2 (2%)
	GW-SW	4.7 (7%)	3.7 (5%)
	GW-SW interactions	4.2 (7%)	1.1 (2%)
	Mixing	3.7 (6%)	2.9 (4%)
	Full	2.8 (4%)	3.4 (5%)

The predictors' importance for individual vegetation types resembled the general pattern of the overall predictors' importance, however, some differences were observed (Fig. 7). In the Full scenario, a predictor from the "mixing" group was the most important for each vegetation type, however, f_{river} was not always the most important predictor.

In the Magnocaricion vegetation type, the most important predictor was f_{rain} with the mean decrease of accuracy (MDA) of 44% and was followed by e_i (MDA 43%), and f_{snow} (MDA 42%) in the Full scenario (Fig. 7). The f_{river} predictor (MDA 37%) was not distinctively high. In this vegetation type in the Mixing scenario, f_{snow} and f_{rain} were the two most important predictors and $f_{groundwater}$ had the lowest importance. The d predictor importance (MDA 37%) was moderate and accounted for 42% of the f_{snow} importance in the Mixing scenario. The l_1 predictor was the most important in the SW scenario, the second most important in the GW-SW scenario, and the fifth most important in the GW-SW interactions scenario. The importance of l_1 was higher than l_{10} in SW, SW-GW interactions, and Full scenarios.

In the Phragmition vegetation type, the f_{river} predictor was predominant and f_{snow}, f_{rain}, and $f_{groundwater}$ were the next three most important predictors in the Full scenario (Fig. 7). The d predictor (MDA 30%) had similar importance as e (MDA 36%, top predictor from groups other than "mixing"). The l_{10} predictor was the most important in the SW, and GW-SW scenarios, while l_1 was the least important predictor therein. In the GW-SW interactions, the four predictors from the "interactions" group were the most important (mean decrease of accuracy 47–53%).

In the sedge-moss vegetation type, the f_{river} predictor was predominant in the Full scenario and the e_d predictor (MDA 57%) was the second most important (Fig. 7). The $f_{groundwater}$ (MDA 30%) was more important than mean depth to groundwater, h_{gw}, and mean soil saturation, m, however, was less important than all exchange-flux-related predictors. In the SW scenario, h_{sw} and l_1 had negative importance, i.e., the models performed better without these predictors. Effectively, l_{10} was the sole predictor in the SW scenario that was relevant for Phragmition vegetation modeling. In the GW-SW scenario, h_{sw} was the most important predictor and was followed by h_{gw}. In the GW-SW interactions, the h_{gw} (MDA 63%) was the most important predictor, but the importance of e was 0.8 percent points lower.

3.3. Past and future vegetation predictions

A shift in the Magnocaricion and sedge-moss vegetation area was predicted between 1950 and 1960 (Fig. 8). The shift was for 26% of the 1950 area in SW, 21% in GW-SW, 19% in GW-SW interactions, 14% in Full, and 14% in Mixing scenarios for Magnocaricion vegetation type and −17% of the 1950 area in SW, −14% in GW-SW, −12% in GW-SW interactions, −8% in Full, and −8% in Mixing scenarios for the sedge-moss vegetation type. There were no significant trends in the

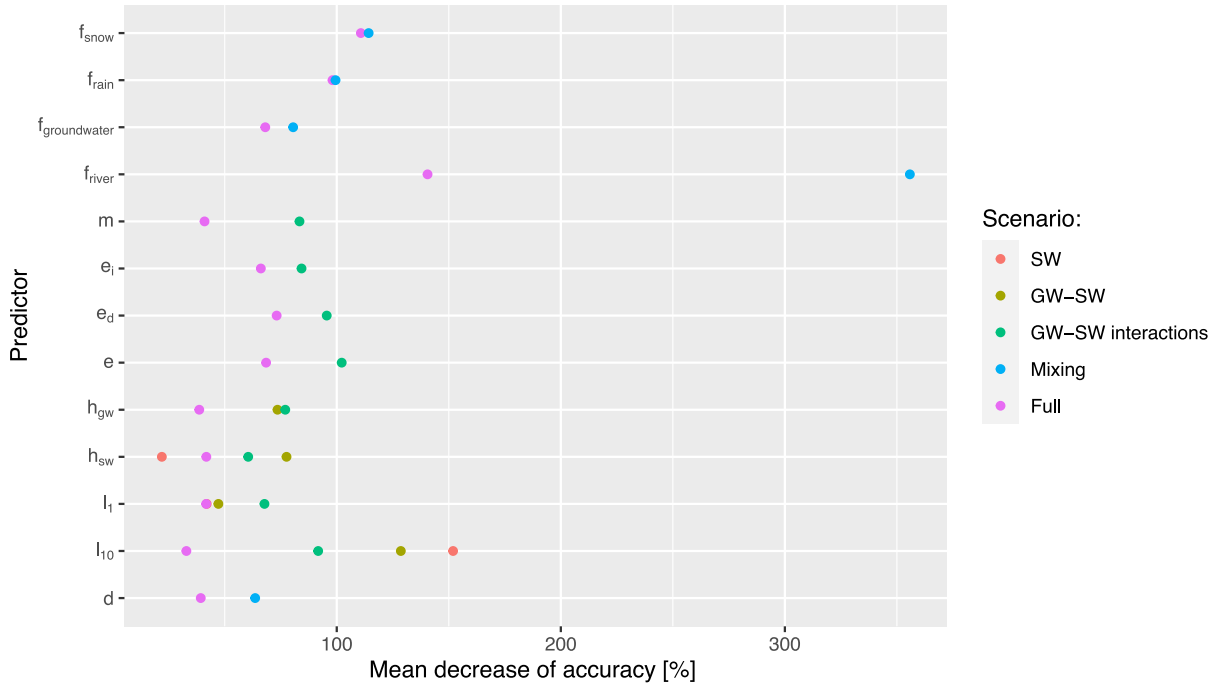

Fig. 6. The predictors' importance quantified by the decrease of accuracy in all vegetation types (overall accuracy) in the fractional approach.

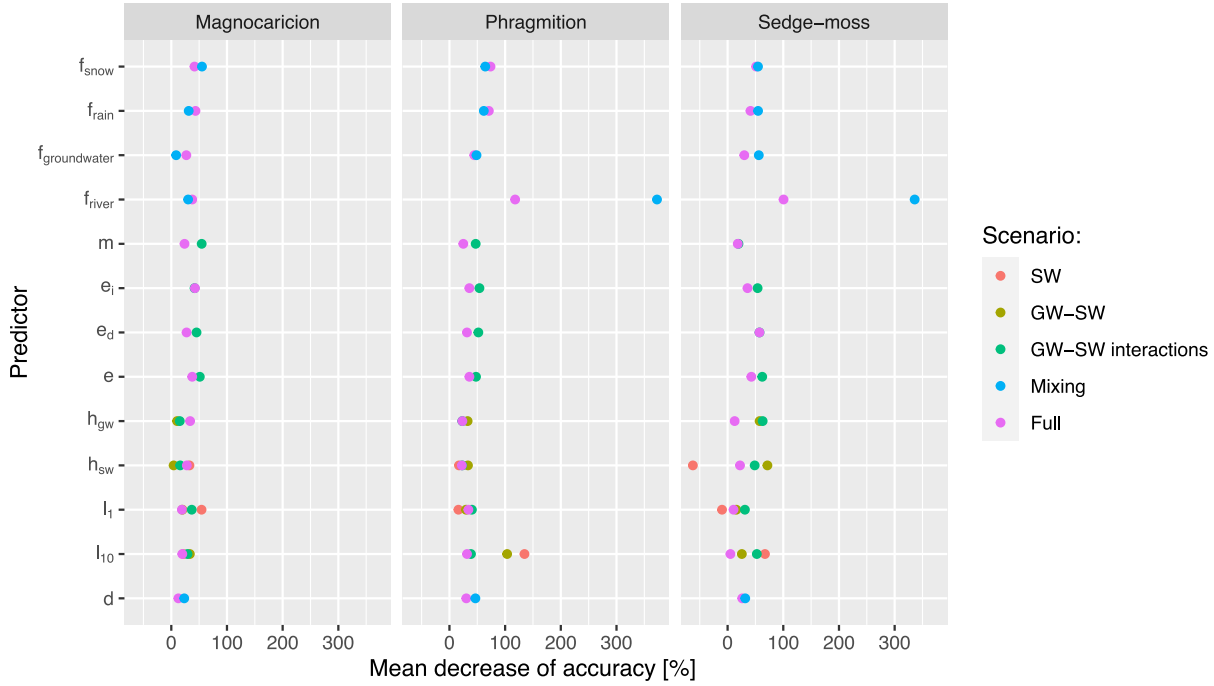

Fig. 7. The predictors' importance quantified by the decrease of accuracy in each vegetation type in the fractional approach.

1910–1950 period, while in the 1960–2010 period for the Magnocaricion vegetation, a significant trend was observed in the Mixing scenario (-0.061 $km^2 year^{-1}$, $p = 0.037$).

Response of the predicted vegetation area varied with the RCP and predictors scenarios for the future period (Fig. 9). The highest Magnocaricion area was predicted for Mixing and Full scenarios, and the lowest for SW and GW-SW, with GW-SW interactions in between. For the sedge-moss vegetation, the situation was the opposite, but the area predicted for GW-SW interactions aligned with SW and GW-SW. In the case of Phragmition vegetation, each scenario predicted a similar area except for GW-SW interactions, which were lower than the remaining scenarios.

Under RCP 2.6 the vegetation area was predicted to be stable over time with a significant trend observed only for sedge-moss vegetation in the Full scenario (-0.039 $km^2 year^{-1}$, $p = 0.014$). Under RCP 4.5 Magnocaricion vegetation area shows significant trends in GW-SW interactions (0.023 $km^2 year^{-1}$, $p = 0.021$), Mixing (0.085 $km^2 year^{-1}$, $p < 0.001$), and Full (0.023 $km^2 year^{-1}$, $p = 0.014$) scenarios. The sedge-moss vegetation area had significant trends in the Mixing scenario (-0.093 $km^2 year^{-1}$, $p < 0.001$). In RCP 8.5 the Magnocaricion vegetation

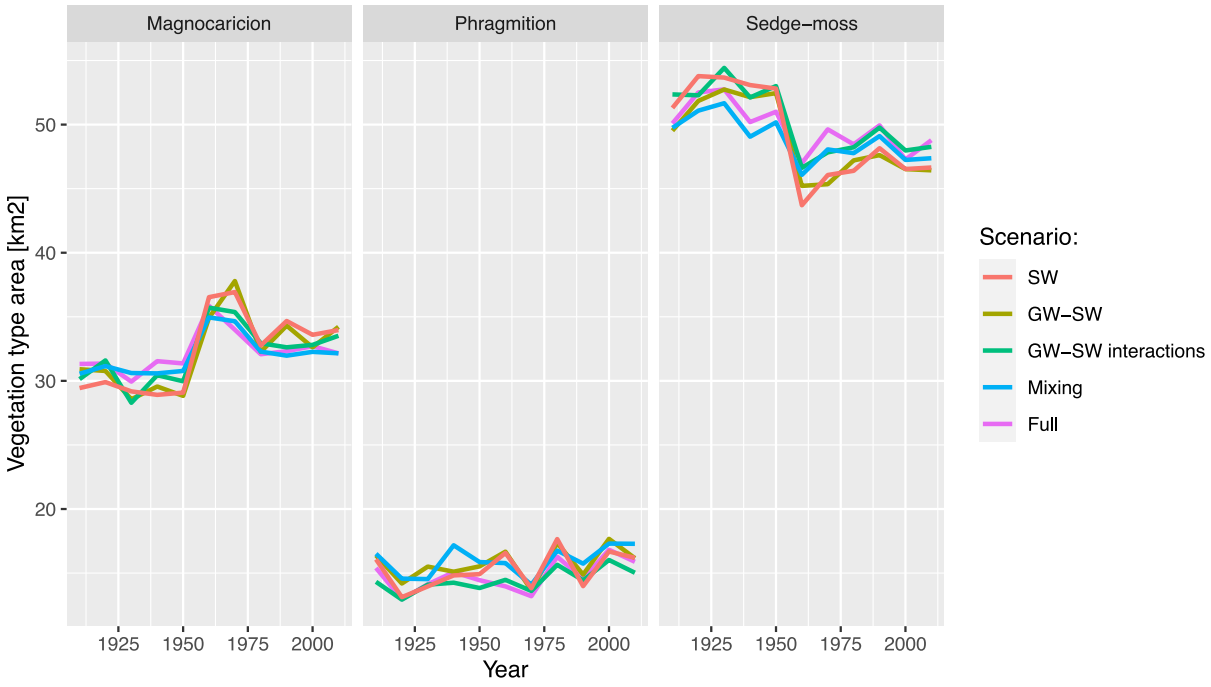

Fig. 8. Predicted vegetation area for the 1910–2010 period. Predictors in each scenario were simulated using IHM forced with the 20CR data for the period 1902–2010.

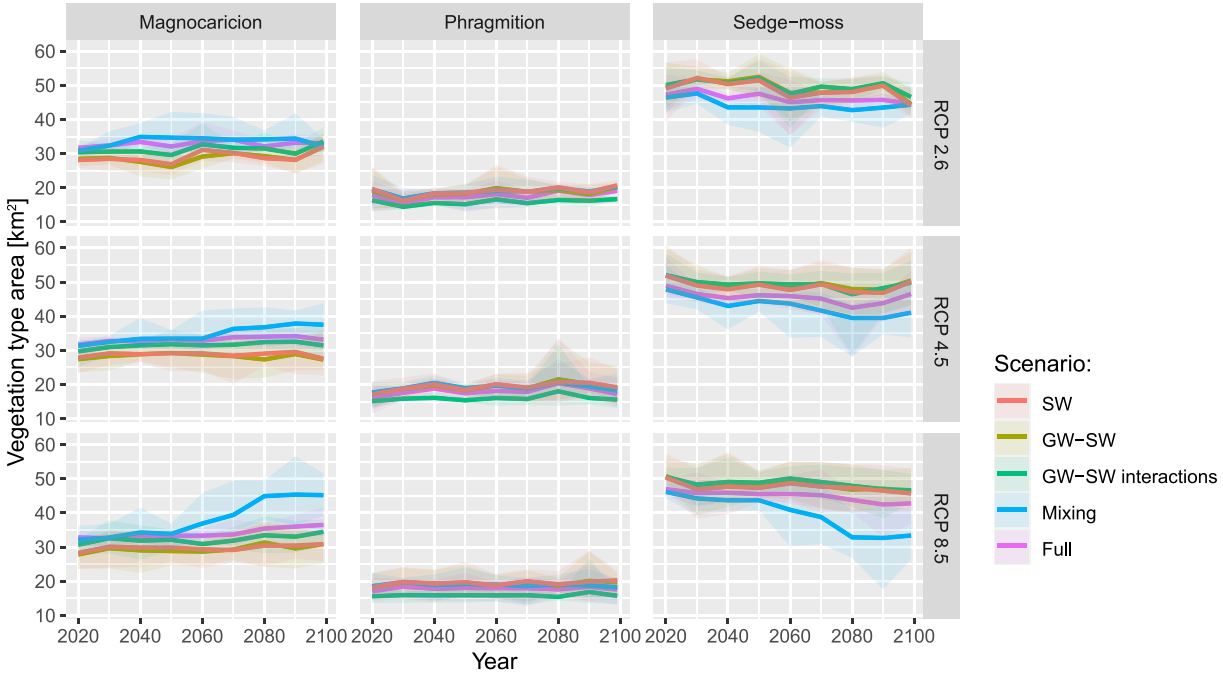

Fig. 9. Predicted vegetation area for the 2020–2099 period. Predictors in each scenario were simulated using IHM forced with the bias-corrected EURO-CORDEX ensemble for RCP 2.6 (5 models), 4.5 (10 models), and 8.5 (10 models) data for the period 2012–2099. Lines represent the mean and ribbons represent 2.5–97.5% ranges of the vegetation area ensembled predictions.

area shows a significant trend for SW (0.020 $km^2 year^{-1}$, $p = 0.046$), GW-SW (0.028 km^2year-1, $p = 0.031$), GW-SW interactions (0.032 $km^2 year^{-1}$, $p = 0.025$), Mixing (0.196 $km^2 year^{-1}$, $p < 0.001$), and Full (0.050 $km^2 year^{-1}$, $p < 0.001$) scenarios. Opposite significant trends were observed for Sedge-moss vegetation area in SW (-0.033 $km^2 year^{-1}$, $p = 0.042$), GW-SW (0.038 $km^2 year^{-1}$, $p = 0.017$), GW-SW interactions (0.037 $km^2 year^{-1}$, $p = 0.017$), Mixing (0.189 $km^2 year^{-1}$, $p < 0.001$), and Full (0.053 $km^2 year^{-1}$, $p < 0.001$) scenarios (Fig. 9).

Predicted vegetation maps for the historical period primarily vary in the degree of spatial scatter in the homogeneous vegetation patches which were less present in the Mixing and Full scenarios than in the remaining scenarios (Fig. 10). The Phragmition belt around the river was the widest and most continuous in the Full scenario map. A similar situation was observed for Mixing and GW-SW interactions (more spatially scattered) while for SW and GW-SW the Phragmition belt was less continuous and narrower. In SW and GW-SW scenario Phragmition

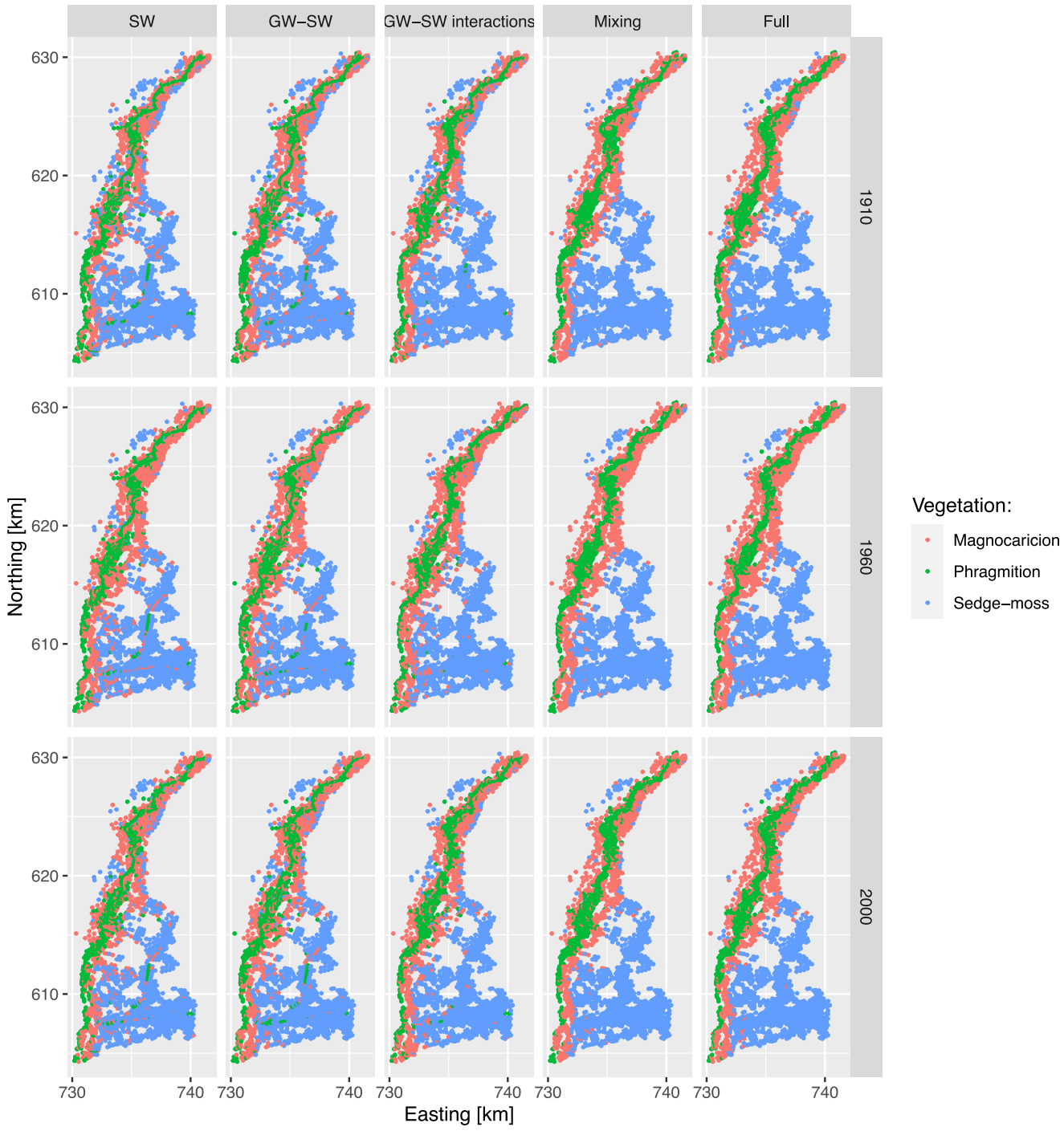

Fig. 10. Predicted vegetation in the IHM nodes for 1910, 1960, and 2000. Nodes, which had forest, or unknown vegetation in 1960, 1980, or 2000 vegetation maps were removed.

and Magnocaricion vegetation was predicted along local relief denivelation such as ditches in the central part of the floodplain, within the sedge-moss patch. The major difference in vegetation distribution between 1960 and 2000 was the narrowing of the Magnocaricion patch by replacement with sedge-moss vegetation in the southern part of the floodplain and at the eastern margin of the northern part of the floodplain.

The predicted vegetation maps for the future period varied in the vegetation types distribution in the analyzed RCP (Fig. 11). In the RCP 2.6 scenario, the differences between predictors scenarios were similar to those observed for the historical period, i.e., less smaller spatially scattered patches within homogeneous vegetation patches and a wider Phragmition continuous belt around the river in the Mixing and Full scenarios than in the SW, GW-SW, and GW-SW interactions scenarios. The width of the Phragmition belt was consistent between the analyzed RCPs within the same predictor scenario. In the SW, GW-SW, and GW-SW interactions scenarios in RCP 4.5 the boundary between Sedge-moss and Magnocaricion vegetation was located closer to the river (up to 300 m) than in RCP 2.6. In RCP 8.5 the Sedge-moss and Phragmition boundary was located nearly as in RCP 2.6 in these scenarios. In the Full scenario, the Sedge-moss and Magnocaricion boundary shift was nearly not observable between RCP 2.6 and RCP 4.5, but in the RCP 8.5, the boundary was located further from the river (up to 300 m) when compared to RCP 2.6. In the Mixing scenario, large patches of

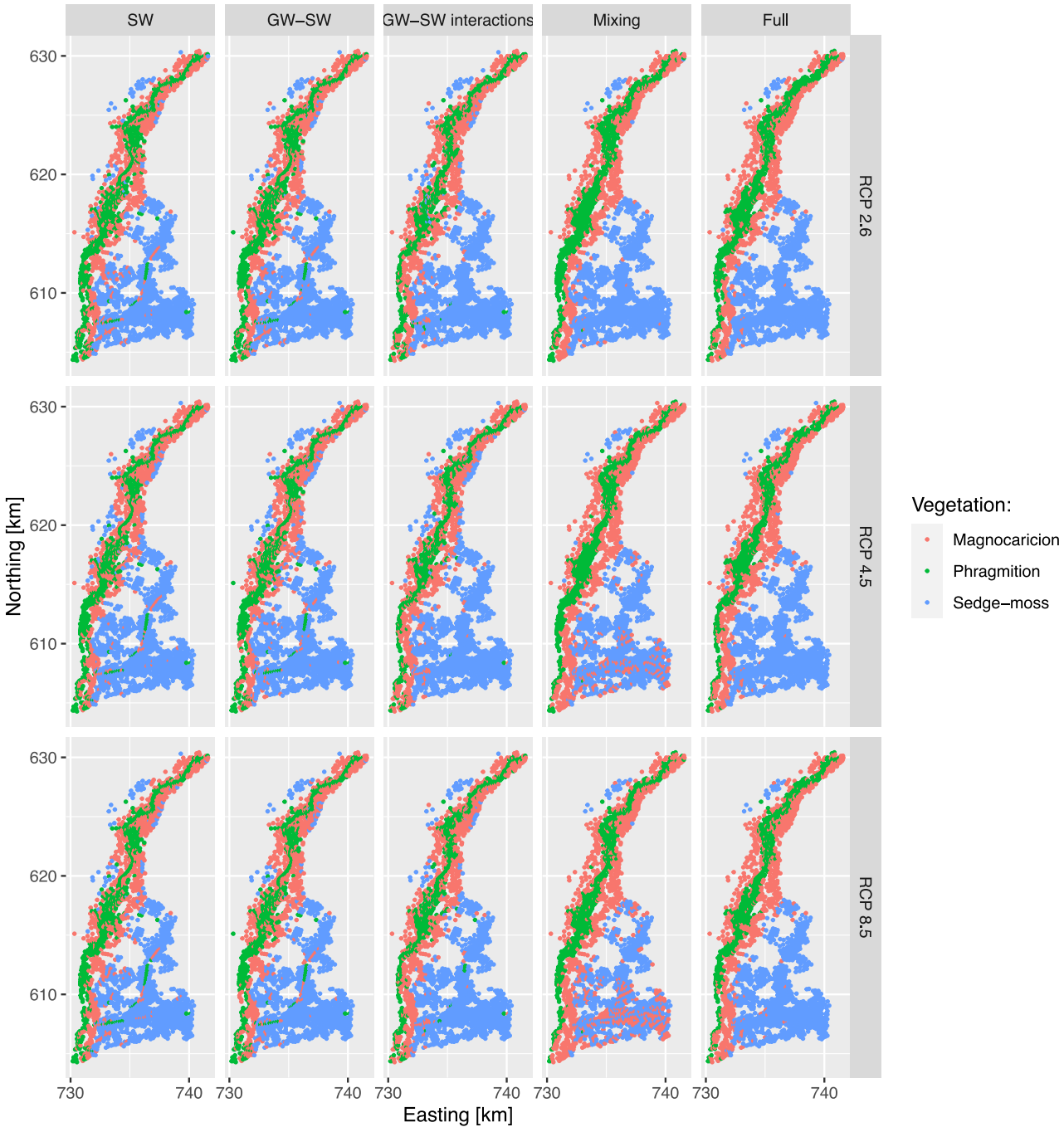

Fig. 11. Predicted vegetation in the IHM nodes for 2099 in RCP 2.6, 4.5, and 8.5 ensembles. Vegetation in each model node was selected based on majority voting in each RCP ensemble. Nodes, which had forest, or unknown vegetation in 1960, 1980, or 2000 vegetation maps were removed.

Magnocaricion vegetation were predicted within the sedge-moss vegetation in the RCP 4.5 and 8.5. More Magnocaricion patches were predicted in RCP 8.5 than in RCP 4.5. The patches were located primarily along the major ditches (up to 600 m belt) in the central part of the floodplain, but not in the ditches themselves.

4. Discussion

4.1. Modelling scenarios validation

We used two approaches for the validation of the vegetation models. The fractional approach, which is most often used due to limited data availability, gives more optimistic accuracy estimates than the OAT approach. This is because a fraction of each map is used for training, hence each map is at least partially known to the classifier. In the OAT approach, the accuracy estimates are more realistic because a map not used for training is used for validation. Our results show in nearly all cases that the accuracy of the vegetation model was higher in the fractional than in the OAT approach. On the other hand, the accuracy differences were not significant, and the pattern of accuracy was very alike for the fractional and OAT approaches. We observed similarities between fractional and OAT approaches results also in the F1 score and areas of vegetation types. Therefore, in our opinion, the fractional approach provides a reasonable insight into the model performance even though the model accuracy is overestimated.

The biggest disagreement between the results from the fractional and

OAT model was the difference between observed and predicted vegetation area. The difference comes from the fact the IHM grid is irregular and the area representative for individual nodes is not the same and effectively some nodes contribute more to the errors in the predicted vegetation area than others. Both OAT and fractional approaches are sensitive to this. However, the effect of an uneven node area was more pronounced in the fractional approach, because the total vegetation area used for validation is smaller than in the OAT approach.

Model performance in terms of accuracy and F1 score improved with the model complexity. The lowest accuracy and F1 scores were achieved by SW and GW-SW scenarios, inclusion of the exchange flux and soil moisture predictors moderately improved the performance in the GW-SW interactions scenario, and the highest performance was obtained by the Full scenario, which additionally used the surface water sources extent. We estimated the accuracy and F1 score in the OAT validation approach, hence it is unlikely that increased model complexity led to overfitting and that F1 scores were overestimated. The pattern of improved performance with increased complexity was not confirmed by the Mixing scenario (only predictors from the "mixing" group), which was benchmarked very close to the Full scenario. The predictors from the "mixing" group were calculated using the HMC method based on the same water fluxes that drive predictors in the "surface", "groundwater", and "interactions" groups. Therefore a reason for the comparable performance of the Mixing and Full scenario could be that the predictors from the "mixing" group integrate the effect of relevant water fluxes and allow the production of similar information with a lower number of predictors.

Another reason why the scenarios which used the predictors from the "mixing" group had the highest accuracy and F1 score is the ability of these predictors to spatially realistically distribute the effect of local hydrological processes. An example of such a distribution is the throughflow in the groundwater domain (Van Loon et al., 2009), which produces a mix of precipitation and groundwater away from the groundwater discharge area. Our IHM simulations showed that the distribution of discharged groundwater, or precipitation water occurs also in inundated conditions and that the continuous inundation is a product of river water with water originating from the floodplain (Berezowski et al., 2019; Berezowski and Partington, 2023). Standard hydrological predictors, such as water depth, inundation period, and depth to groundwater, or even dynamic predictors, such as exchange flux between groundwater and surface water only reflect the local situation, which is often affected by local relief (locally shallower or deeper surface water or groundwater), and are not able to show the spatial effect of water fluxes over a larger part of the floodplain. Correlation between the zones of water in inundated conditions was identified earlier using field sampling for the Biebrza floodplain (Chormański et al., 2011; Keizer et al., 2014) and our results confirm the relevance of this phenomenon for vegetation development in long-term periods.

Our results showed that vegetation modelling based on surface water predictors only is possible (SW scenario) but is clearly suboptimal. Such an approach has been used in many studies (Todd et al., 2010; Mosner et al., 2015; Yao et al., 2020; Liang et al., 2020), however, recently another comparison of vegetation modelling scenarios showed that using both groundwater and surface water predictors from IHM outperforms simpler vegetation models (Gattringer et al., 2019). This approach is comparable to the GW-SW scenario in our study, which did not have significantly higher accuracy than the SW scenario. Our study, on the other hand, showed that significantly higher accuracy of vegetation modelling can be achieved when the exchange flux and soil moisture are used as predictors as in the GW-SW interactions scenario. Although the GW-SW interactions scenario did not perform as well as the Full scenario, this highlights that if the water sources extents from a method like HMC are not available at least interactions between groundwater and surface water should be used as predictors for floodplain vegetation modelling.

A number of studies conducted time-varying floodplain vegetation modelling with basic hydrological predictors only. A study conducted in Dongting Lake, China, showed that surface water hydrological predictors derived for different flooding phases are correlated with reeds or sedge vegetation cover (Peng et al., 2022). Another study carried out in the Mitchell River catchment, Australia, showed that the floodplain vegetation productivity can be explained by the hydrological and meteorological forcing variability (Ndehedehe et al., 2021). Similarly, a study carried out in Karnali River, Nepal, has shown that hydrological and climatic variables, along with abiotic factors can explain grassland vegetation change (Bijlmakers et al., 2023). There are two explanations why these studies were successfully conducted without water sources extent predictors. First, these studies analyzed vegetation or productivity figures lumped over these floodplains area, whereas our analysis was conducted spatially to show where the shift of vegetation types would occur. The lack of spatial aspect allowed to relate vegetation properties, to river discharge or water levels, which are related to the abundance of river water. Effectively, these hydrological variables could be a proxy for the river water source extent, which as shown in our results, is the most important predictor. The second explanation is that in spite of the Biebrza floodplain being a reference site for wetlands research, not all wetlands are shaped by the same hydrological processes. Indeed, the aforementioned studies were conducted over different climatic zones, which could be another reason why the influence of rainfall, snowmelt, and groundwater extents in the inundation were less relevant.

4.2. Predictors importance

Overall the most important predictor in the Full scenario was the f_{river}, which identifies the extent of the river water in the inundation. The f_{river} predictor was two to three times more important than the next most important predictors for overall model accuracy and Phragmition and Sedge-moss vegetation type. Scenarios, which used f_{river} (and other predictors from the "mixing" group) had an overall accuracy of 5 percent points higher than the GW-SW interactions scenario. This shows the relevance of the river water zone and its interactions with atmospheric water from rainfall and snowmelt, and discharged groundwater in shaping the vegetation in the Biebrza floodplain.

The high importance of f_{river} for the Phragmition vegetation is in line with other studies indicating that high productive vegetation is present in the river water zone (Chormański et al., 2011; Keizer et al., 2014). Several earlier studies showed that the vegetation zonation in the Biebrza floodplain is related to flood frequency, or inundation length (Okruszko et al., 2010; Grygoruk et al., 2021). We do not question that because flooding was primarily driven by the river water, and the extent of the river water is correlated to these variables in the proximity of the river. Simple SW and GW-SW scenarios showed that inundation length or surface mean water depth were important predictors for Phragmition and Magnocaricion vegetation. However, the scenarios which used the "mixing" group predictors explained the vegetation pattern much better. This gives additional evidence to support earlier findings that the extent of water from different sources shapes the vegetation pattern in the Biebrza floodplain.

However, the f_{river} predictor was not the most important for Magnocaricion vegetation, which is also a highly productive vegetation type (Wassen et al., 2002). The Magnocaricion zone is located as a transient zone between Phragmition and Sedge-moss vegetation and hence is influenced by hydrological conditions characteristics for both vegetation types. Both in Phragmition and Sedge-moss f_{river} was important, but except that the groundwater-related predictors were important in Sedge-moss (e_i, e, e_d, $f_{groundwater}$) and the surface-water-related predictors were important for Phragmition (l_1, l_{10}). The transient character of Magnocaricion was reflected in the predictors' importance pattern in the Full scenario, which showed that predictors from all groups are important at a similar level. This makes the modeling of Magnocaricion vegetation more challenging than Phragmition and Sedge-moss, which was

reflected by lower F1 scores for this vegetation type.

The IHM simulations with the HMC method have shown that high d values are associated with the decrease of water velocity due to contact of river water with floodplain water (Fig. 12). The decrease in water velocity leads to particulate sediment deposition, which was identified as a better predictor of highly productive vegetation in the Biebrza floodplain than the extent of the river water zone (Keizer et al., 2018). We expected that the d predictor would receive higher importance, while it was only moderately important for Phragmition and Magnocaricion in the Full scenario. The reason for this can be twofold. First, the d predictor is calculated based on the remaining fractions predictors from the mixing "group" (see description in Table 1), hence it provided redundant information for the random forest classifier. Second, the d predictor shows a boundary between the river and floodplain water, which is very informative when context from neighboring nodes is provided for the model but may not be necessarily informative when model training is performed on individual nodes as in our case.

4.3. Past and future vegetation predictions

The unrealistic shift in the predicted vegetation area between 1950 and 1960 shows the major drawback of the vegetation modeling methodology presented in this study. The empirical model is driven by data, not by processes, therefore will suffer from the quality of the data. Even though we used the IHM (physical hydrological model), which was validated using water levels since 1881 (with gaps) the produced predictors clearly showed different distributions before and after 1950. The validation of IHM was however much more extensive in the 1950–2019 period than before 1950. Also, IHM simulations and 20CR forcing data showed similar statistics when compared against EURO-CORDEX and observations data in the 1970–2005 period (Berezowski and Partington, 2023). We were not able to compare the 20CR forcing data against observation for the period before 1950 due to the lack of continuous meteorological data in our study area. The 20CR product had increased RMSE of atmospheric pressure in the northern hemisphere in the pre-1950 period in reference to the post-1950 period that was in line with the increase of the number of observations used in the product from approximately 200–1000 (1880–1950) to 1000–3000 (1950–2008) (Slivinski et al., 2019). Therefore, we believe that the shift in the predicted vegetation area was primarily due to the pre-1950 lower quality of 20CR forcing data used in the IHM that effectively produced a narrower distribution of several predictors in that period in comparison to the post-1950 period (Figure S1).

We observed a decreasing trend in the 1960–2010 period only for the Magnocaricion vegetation area in the Mixing scenario, which was in line with the decreased area of this vegetation in subsequent maps from 1960 to 2000. In the future period, 2020–2099, the predicted trend for the Magnocaricion area had an opposite direction namely increasing. This could be due to only six predicted maps used to calculate the trend in the 1960–2010 period and the fact the beginning of this period was characterized by higher error (as discussed in the previous paragraph). Another explanation is a flaw in the predictions in the Mixing scenario, which had high accuracy and F1 scores but also was characterized by the highest difference of predicted vegetation area for Magnocaricion. The mixing scenario also predicted big changes in Magnocaricion vegetation under RCP 4.5 and RCP 8.5 by the end of the century which was not in line with other scenarios. Notably, these deviations were not present in the Full scenario, which also used the predictors from the "mixing" group. This shows that although the Mixing scenario relatively well explained the vegetation pattern during relatively stable hydrological conditions (1960–2010) it was underconstrained (by lack of standard hydrological predictors such as surface water depth) for predictions in the far future under climate change.

Each scenario predicted significant trends in vegetation area under RCP 8.5. This was not the case in less extreme scenarios RCP 2.6 and RCP 4.5, where simple scenarios GW and GW-SW did not predict any trends.

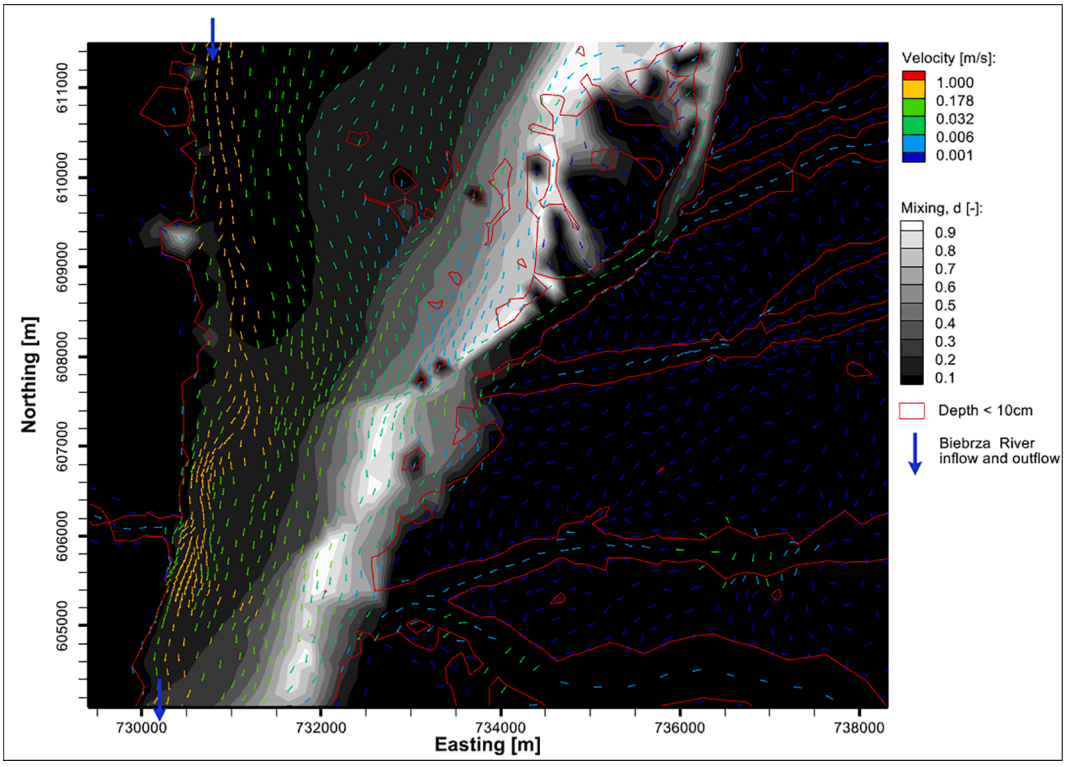

Fig. 12. Degree of mixing between river water and floodplain water (i.e. groundwater discharge, rainfall, and snowmelt) simulated with the IHM and HGS methods during a spring flood event on 27th of March 2005 in a southern section of the floodplain. High d values indicate similar proportions of river and floodplain water, i.e. presence of mixing, and low values indicate that one source dominates over another, i.e. no mixing (see Table 1). The color of the velocity vectors is proportional to the water velocity (the length of each vector is the same).

This suggests that the simple scenarios had lower accuracy and F1 scores than scenarios with more predictors because of fit-to-average hydrological conditions, which reflect the observed vegetation pattern that overlaps in all three maps used for training. Because of that a very strong shift in hydrological conditions, such as in RCP 8.5, has to be present to force the prediction of trends in SW and GW-SW scenarios.

The inclusion of predictors for the "interactions" group in the GW-SW interactions scenario improved the accuracy and F1 score in reference to the SW and GW-SW scenarios. The vegetation area predicted in the GW-SW interactions scenario was also more sensitive to future climate changes than in the SW and GW-SW scenarios. We observed the difference between the Full and GW-SW interactions primarily in the spatial scatter (spatially separated relatively small patches) in the predicted vegetation. We attribute the decrease of spatial scatter in the Full scenario to the predictors representing fractions of different water sources in the inundation. First, in comparison to the surface water depth, or depth to groundwater the water source extent predictors are less affected by local relief, hence less spatial scatter. Second, these predictors present continuous areas with the dominant (or mixed) water source which is the effect of water transport during inundated conditions. This forms a spatial extent of a given water source and is associated with its chemical and physical (e.g. sediments) properties that help the model to predict continuous vegetation zones.

Vegetation models similar to the one presented in this study can be used as a decision-support tool for floodplain management (Leyer, 2005; Świątek et al., 2008; Mosner et al., 2011; Mosner et al., 2015). Our results show that management decisions based on simple vegetation models (only groundwater and\or surface water predictors) would be less accurate and would often wrongly indicate areas with changed vegetation in comparison to models additionally using the exchange flux and soil moisture (GW-SW interactions scenario), and water sources extent (Full scenario). The wrongly indicated areas in simple scenarios would occur in distanced areas from a water source (e.g. from a river), that is characterized by similar surface water depth or depth to groundwater as near to the source due to local relief (small pits or elevations, dikes) but do not have contact with the source. Therefore, for management support, especially in longer temporal horizons, we recommend using models that are based on predictors that reflect conditions that limit vegetation development, e.g. the provision of nutrients, what can be realized using the water sources extent.

4.4. Limitations of this study

Validation figures and vegetation predictions suffer from several limitations due to the methodology of this study. First, the earlier vegetation maps were conducted without access to geographical information systems and satellite navigation technology which could decrease the accuracy of the vegetation patches. Effectively the difference in the vegetation patch areas between the maps could have been not only due to hydrological conditions bat also due to mapping error. Second, the IHM, although validated against a number of spatiotemporal data sets (Berezowski and Partington, 2023), had some errors. Effectively this error was propagated to the predictors used for the vegetation modelling and affected the results. Third, the model analyzed only the effect of the hydrological conditions (which changed due to climatic forcing) while neglecting other factors affecting vegetation. Primarily this could be human management of the floodplain area (a.o. harvesting of vegetation, grazing), which although small (see Section 2.1), was present. Mowing, grazing, and construction of small dams to increase water retention were conducted (Berezowski et al., 2018) and could, to some extent, be responsible for vegetation changes. Finally, the machine learning model for vegetation was data-driven. Therefore, the predictions (especially for longer time horizons) made by the model are affected by the data quality. In this study, we identified some unrealistic vegetation area predictions that could be attributed to the IHM forcing data quality pre-1950, however, for the future climate period the IHM forcing data quality may also affect the vegetation modelling results.

5. Summary and conclusions

Our vegetation model scenarios showed that the inclusion of the "mixing" predictors, i.e., the extent of such water sources as river water, discharged groundwater, rainfall, and snowmelt during inundated conditions significantly improve the accuracy of floodplain vegetation models in reference to standard hydrological predictors, what supports the hypothesis of this research. We observed the water sources extent predictors effect in:

1. Spatial distribution of local hydrological processes, e.g. groundwater influenced inundation based on local groundwater discharge. This allows the delineation of an area in which water with particular chemical, or physical properties (e.g. calcareous groundwater, nutrient-poor rainwater) is in contact with vegetation.
2. Development of zones predominated by a single water source that is more continuous than standard hydrological variables such as mean water depth. This continuity of predictors allows the model to predict the vegetation patches more realistically with less spatial scatter associated to local relief.
3. Identification of the river water (nutrient-rich) extent which is a better predictor of the highly productive vegetation in the floodplain than mean water depth, or inundation length.

We showed that floodplain vegetation can also be modeled with standard hydrological variables. In such a case the modeling scenario which included interactions between groundwater and surface water outperformed in terms of accuracy simple models, which used depth to groundwater, surface water depth, and length of the inundation predictors only. Our predictions forced by future climate showed that the simplest models were likely fitting to the average hydrological conditions of the past, therefore they were not able to predict trends in areas covered by a certain vegetation for the future simulations. The predictions forced by future climate also showed that the scenario, which used only the water sources extent predictors predicted a vegetation pattern that was not reproduced by any other scenario. This was likely due to the under-constrain of this model scenario by lack of standard hydrological variables since the Full scenario, which used both water sources extent and standard predictors not only had the highest accuracy, and was able to predict future trends, but also predicted a future vegetation pattern that was realistic. Furthermore, our experiments showed the drawback of the data-driven modeling approach by predictions of unrealistic vegetation areas before 1960, which was due to the lower quality of predictors in that period. In spite of that, the models performed well in periods of good forcing data quality. Therefore our general recommendation is to support management decisions with vegetation models which include predictors that precisely reflect conditions that limit vegetation development (e.g. by nutrient supply), i.e. the spatial extent of certain water sources during the inundation, rather than models that use only inundation depth, length of the inundation, or depth to groundwater. The latter are affected by local relief and do not reflect the physical and chemical properties of the water.

Our research compared two methods of model validation. The fractional approach which is more popular due to limited multi-temporal data availability indicated higher accuracy than the OAT approach. While the OAT accuracy was more realistic, the accuracy differences between two approaches were not significant, and the pattern of accuracy was very alike for the fractional and OAT approaches.

CRediT authorship contribution statement

Tomasz Berezowski: Conceptualization, Methodology, Software, Formal analysis, Investigation, Resources, Data curation, Writing – original draft, Writing – review & editing, Visualization, Project

administration, Funding acquisition. **Martin Wassen:** Conceptualization, Methodology, Writing – review & editing.

Declaration of Competing Interest

The authors declare that they have no known competing financial interests or personal relationships that could have appeared to influence the work reported in this paper.

Acknowledgment

This research was supported by grant: 2017/26/D/ST10/00665 funded by the National Science Centre, Poland. The vegetation map was provided by the Biebrza National Park, the map is available upon request from the owner; we thank the Biebrza National Park for the permission for field measurements in the Park area. Hydrological predictors and processed vegetation maps used in this research are available in https://doi.org/10.34808/3afh-7h82 (Berezowski, 2023). We thank two anonymous reviewers for their comments which led to the improvement of this paper.

Appendix A. Supplementary data

Supplementary data to this article can be found online at https://doi.org/10.1016/j.ecolind.2023.110854.

References

Almendinger, J.E., Leete, J.H., 1998. Peat characteristics and groundwater geochemistry of calcareous fens in the Minnesota River Basin, U.S.A. Biogeochemistry 43, 17–41. https://doi.org/10.1023/a: 1005905431071.

Anderson, O., Harrison, A., Heumann, B., Godwin, C., Uzarski, D., 2023. The influence of extreme water levels on coastal wetland extent across the laurentian great lakes. Sci. Total Environ. 885, 163755 https://doi.org/10.1016/j.scitotenv.2023.163755.

Banaszuk, H., 2004. Biebrza Basin and Biebrza National Park. Ekonomia i Środowisko, Bialystok, Poland. In Polish.

Benjankar, R., Egger, G., Jorde, K., Goodwin, P., Glenn, N.F., 2011. Dynamic floodplain vegetation model development for the Kootenai River, USA. J. Environ. Manage. 92, 3058–3070. https://doi.org/10.1016/j.jenvman.2011.07.017.

Berezowski, T., Partington, D., 2023. Impact of climate change on water sources and riverfloodplain mixing in the natural wetland floodplain of Biebrza River - preprint. Authorea. https://doi.org/10.22541/essoar.167898498.81970799/v1.

Berezowski, T., Wassen, M., Szatyłowicz, J., Chormański, J., Ignar, S., Batelaan, O., Okruszko, T., 2018. Wetlands in flux: looking for the drivers in a central European case. Wetl. Ecol. Manag. 26 (5), 849–863.

Berezowski, T., Partington, D., Chormanski, J., Batelaan, O., 2019. Spatiotemporal dynamics of the active perirheic zone in a natural wetland floodplain. Water Resour. Res. 55, 9544–9562. https://doi.org/10.1029/2019wr024777.

Berezowski, T., 2023. Hydrological predictors used for vegetation modelling in the lower Biebrza valley 1900-2099 . doi:10.34808/3afh-7h82. Gdansk University of Technology, Gdansk, Poland.

Beumer, V., van Wirdum, G., Beltman, B., Griffioen, J., Verhoeven, J.T.A., 2007. Biogeochemical consequences of winter flooding in brook valleys. Biogeochemistry 86 (1), 105–121.

Bijlmakers, J., Griffioen, J., Karssenberg, D., 2023. Environmental drivers of spatio-temporal dynamics in floodplain vegetation: grasslands as habitat for megafauna in Bardia National Park (Nepal). Biogeosciences 20, 1113–1144. https://doi.org/10.5194/bg-20-1113-2023.

Blom, C., Voesenek, L., 1996. Flooding: the survival strategies of plants. Trends Ecol. Evol. 11, 290–295. https://doi.org/10.1016/0169-5347(96)10034-3.

Breiman, L., 2001. Random forests. Machine Learning 45, 5–32. https://doi.org/10.1023/a:1010933404324.

Brewer, S.K., Worthington, T.A., Mollenhauer, R., Stewart, D.R., McManamay, R.A., Guertault, L., Moore, D., 2018. Synthesizing models useful for ecohydrology and ecohydraulic approaches: An emphasis on integrating models to address complex research questions. Ecohydrology 11 (7). https://doi.org/10.1002/eco.1966.

Capon, S., 2005. Flood variability and spatial variation in plant community composition and structure on a large arid floodplain. J. Arid Environ. 60, 283–302. https://doi.org/10.1016/j. jaridenv.2004.04.004.

Chormanski, J., Okruszko, T., Ignar, S., Batelaan, O., Rebel, K.T., Wassen, M.J., 2011. Flood mapping with remote sensing and hydrochemistry: a new method to distinguish the origin of flood water during floods. Ecol. Eng. 37 (9), 1334–1349.

Dang, X., Huai, W., Zhu, Z., 2022. Numerical simulation of vegetation evolution in compound channels. Environ. Sci. Pollut. Res. 30, 1595–1610.

Dwire, K.A., Kauffman, J.B., Baham, J.E., 2006. Plant species distribution in relation to water-table depth and soil redox potential in montane riparian meadows. Wetlands 26, 131–146. https://doi.org/10.1672/0277-5212(2006)26[131:PSDIRT]2.0.CO;2.

Ellery, W.N., Ellery, K., Mccarthy, T.S., 1993. Plant distribution in islands of the Okavango Delta, Botswana: determinants and feedback interactions. Afr. J. Ecol. 31, 118–134. https://doi.org/10.1111/j.1365-2028.1993.tb00526.x.

Eurostat, 2019. EUROPOP2019 - Population projections at regional level (2019-2100).

Fernandes, M.R., Segurado, P., Jauch, E., Ferreira, M.T., 2016. Riparian responses to extreme climate and land-use change scenarios. Sci. Total Environ. 569–570, 145–158. https://doi.org/10.1016/j.scitotenv.2016.06.099.

Ferreira, L.V., Stohlgren, T.J., 1999. Effects of river level fluctuation on plant species richness, diversity, and distribution in a floodplain forest in Central Amazonia. Oecologia 120, 582–587. https://doi.org/10.1007/s004420050893.

Fox, E.W., Hill, R.A., Leibowitz, S.G., Olsen, A.R., Thornbrugh, D.J., Weber, M.H., 2017. Assessing the accuracy and stability of variable selection methods for random forest modeling in ecology. Environ. Monit. Assess. 189 https://doi.org/10.1007/s10661-017-6025-0.

Gattringer, J.P., Maier, N., Breuer, L., Otte, A., Donath, T.W., Kraft, P., Harvolk-Schoning, S., 2019. Modelling of rare flood meadow species distribution by a combined habitat surface watergroundwater model. Ecohydrology 12, e2122.

Glaser, B., Hopp, L., Partington, D., Brunner, P., Therrien, R., Klaus, J., 2021. Sources of surface water in space and time: Identification of delivery processes and geographical sources with hydraulic mixing-cell modeling. Water Resour. Res. 57 https://doi.org/10.1029/2021wr030332.

Gnatowski, T., Szatyłowicz, J., Brandyk, T., Kechavarzi, C., 2010. Hydraulic properties of fen peat soils in Poland. Geoderma 154 (3-4), 188–195.

Grootjans, A., Adema, E., Bleuten, W., Joosten, H., Madaras, M., Janakova, M., 2006. Hydrological landscape settings of base-rich fen mires and fen meadows: an overview. Appl. Veg. Sci. 9, 175–184. https://doi.org/10.1111/j.1654-109x.2006.tb00666.x.

Grygoruk, M., Kochanek, K., Mirosław-Świątek, D., 2021. Analysis of long-term changes in inundation characteristics of near-natural temperate riparian habitats in the lower basin of the Biebrza valley, Poland. J. Hydrol.: Regional Stud. 36, 100844 https://doi.org/10.1016/j. ejrh.2021.100844.

Gutierrez-Jurado, K.Y., Partington, D., Batelaan, O., Cook, P., Shanafield, M., 2019. What triggers streamflow for intermittent rivers and ephemeral streams in low-gradient catchments in Mediterranean climates. Water Resour. Res. 55, 9926–9946. https://doi.org/10.1029/2019wr025041.

Hollander, M., Wolfe, D.A., Chicken, E., 2015. Nonparametric Statistical Methods. Wiley.

Houzé, C., Durand, V., Mügler, C., Pessel, M., Monvoisin, G., Courbet, C., Noûs, C., 2022. Combining experimental and modelling approaches to monitor the transport of an artificial tracer through the hyporheic zone. Hydrol. Process. 36 (2) https://doi.org/10.1002/hyp.14498.

Hwang, H.T., Park, Y.J., Sudicky, E., Forsyth, P., 2014. A parallel computational framework to solve flow and transport in integrated surface subsurface hydrologic systems. Environ. Model. Softw. 61, 39–58.

Illeperuma, N.D., Dixon, M.D., Elliott, C.M., Magnuson, K.I., Withanage, M.H.H., Vogelmann, J.E., 2023. Spatiotemporal patterns and environmental drivers of eastern redcedar (Juniperus virginiana) abundance along the Missouri River, USA. Landsc. Ecol. 38, 1677–1695. https://doi.org/10.1007/s10980-023-01632-y.

IMGW-PIB, 2019. Public data, period: 1951-2019. URL: https://danepubliczne.imgw.pl/data/dane_pomiarowo_obserwacyjne/. accessed: 2019-04-21.

Jabłońska, E., Pawlikowski, P., Jarzombkowski, F., Chormański, J., Okruszko, T., Kłosowski, S., 2011. Importance of water level dynamics for vegetation patterns in a natural percolation mire (Rospuda fen, NE Poland). Hydrobiologia 674, 105–117. https://doi.org/10.1007/s10750-011-0735-z.

Jacob, D., Petersеń, J., Eggert, B., Alias, A., Christeńseń, O.B., Bouwer, L.M., Brauń, A., Colette, A., Deque, M., Georgievski, G., Georgopoulou, E., Gobiet, A., Menut, L., Nikulin, G., Haensler, A., Hempelmann, N., Jones, C., Keuler, K., Kovats, S., Kroner, N., Kotlarski, S., Kriegsmann, A., Martin, E., van Meijgaard, E., Moseley, C., Pfeifer, S., Preuschmann, S., Radermacher, C., Radtke, K., Rechid, D., Rounsevell, M., Samuelsson, P., Somot, S., Soussana, J.F., Teichmann, C., Valentini, R., Vautard, R., Weber, B., Yiou, P., 2014. EURO-CORDEX: new high-resolution climate change projections for European impact research. Reg. Environ. Chang. 14, 563–578. https://doi.org/10.1007/s10113-013-0499-2.

Jing, L., Zeng, Q., He, K.e., Liu, P., Fan, R., Lu, W., Lei, G., Lu, C., Wen, L.i., 2023. Vegetation dynamic in a large floodplain wetland: The effects of hydroclimatic regime. Remote Sens. (Basel) 15 (10), 2614.

JRC, 2019. Agri4Cast Resources Portal. URL: https://agri4cast.jrc.ec. europa.eu/dataportal/. date accessed: 2019-12-03.

Junk, W.J., Piedade, M.T.F., Schongart, J., Wittmann, F., 2012. A classification of major natural habitats of Amazonian white-water river floodplains (varzeas). Wetl. Ecol. Manag. 20, 461–475.

Junk, W.J., Wittmann, F., Schöngart, J., Piedade, M.T.F., 2015. A classification of the major habitats of Amazonian black-water river floodplains and a comparison with their white-water counterparts. Wetl. Ecol. Manag. 23 (4), 677–693.

Keddy, P.A., 1984. Plant zonation on lakeshores in Nova Scotia: A test of the resource specialization hypothesis. J. Ecol. 72, 797. https://doi.org/10.2307/2259532.

Keizer, F., Schot, P., Okruszko, T., Chormainski, J., Kardel, I., Wassen, M., 2014. A new look at the flood pulse concept: The (ir)relevance of the moving littoral in temperate zone rivers. Ecol. Eng. 64, 85–99.

Keizer, F., der Lee, G.V., Schot, P., Kardel, I., Barendregt, A., Wassen, M., 2018. Floodplain plant productivity is better predicted by particulate nutrients than by dissolved nutrients in floodwater. Ecol. Eng. 119, 54–63.

Kotowski, W., Jabłońska, E., Bartoszuk, H., 2013. Conservation management in fens: Do large tracked mowers impact functional plant diversity? Biol. Conserv. 167, 292–297. https://doi.org/10.1016/j.biocon.2013.08.021.

Laranjeiras, T.O., Naka, L.N., Leite, G.A., Cohn-Haft, M., 2021. Effects of a major Amazonian river confluence on the distribution of floodplain forest avifauna. J. Biogeogr. 48, 847–860. https://doi.org/10.1111/jbi.14042.

Leyer, I., 2005. Predicting plant species' responses to river regulation: the role of water level fluctuations. J. Appl. Ecol. 42, 239–250. https://doi.org/10.1111/j.1365-2664.2005. 01009.x.

Liang, D., Lu, J., Chen, X., Liu, C., Lin, J., 2020. An investigation of the hydrological influence on the distribution and transition of wetland cover in a complex lake-floodplain system using time-series remote sensing and hydrodynamic simulation. J. Hydrol. 587, 125038 https://doi.org/10.1016/j.jhydrol.2020.125038.

Llampazo, G.F., Coronado, E.N.H., del Aguila-Pasquel, J., Oroche, C.J.C., Narvaez, A.D., Huay-macari, J.R., Rws, J.G., Lawson, I.T., Hastie, A., Baird, A.J., Baker, T.R., 2022. The presence of peat and variation in tree species composition are under different hydrological controls in Amazonian wetland forests. Hydrol. Process. 36, e14690.

Matuszkiewicz, A., Głowacka, I., Jakubowski, W., Kaminski, J., Myslinski, G., Sobczyjnski, L., 2000. Conservation Plan for Biebrza National Park. Conservation of land non-forest ecosystems. Biebrza National Park, Osowiec-Twierdza, Poland. In Polish.

Mertes, L.A.K., 1997. Documentation and significance of the perirheic zone on inundated floodplains. Water Resour. Res. 33 (7), 1749–1762.

Mosner, E., Schneider, S., Lehmann, B., Leyer, I., 2011. Hydrological prerequisites for optimum habitats of riparian Salix communities - identifying suitable reforestation sites. Appl. Veg. Sci. 14, 367–377. https://doi.org/10.1111/j.1654-109x.2011.01121.x.

Mosner, E., Weber, A., Carambia, M., Nilson, E., Schmitz, U., Zelle, B., Donath, T., Horchler, P., 2015. Climate change and floodplain vegetation-future prospects for riparian habitat availability along the Rhine River. Ecol. Eng. 82, 493–511. https://doi.org/10.1016/j.ecoleng.2015. 05.013.

Murray-Hudson, M., Wolski, P., Cassidy, L., Brown, M.T., Thito, K., Kashe, K., Mosimanyana, E., 2014. Remote sensing-derived hydroperiod as a predictor of floodplain vegetation composition. Wetl. Ecol. Manag. 23, 603–616. https://doi.org/10.1007/s11273-014-9340-z.

Ndehedehe, C.E., Onojeghuo, A.O., Stewart-Koster, B., Bunn, S.E., Ferreira, V.G., 2021. Upstream flows drive the productivity of floodplain ecosystems in tropical Queensland. Ecol. Ind. 125, 107546 https://doi.org/10.1016/j.ecolind.2021.107546.

Nogueira, G.E.H., Schmidt, C., Brunner, P., Graeber, D., Fleckenstein, J.H., 2021. Transit-time and temperature control the spatial patterns of aerobic respiration and denitrification in the riparian zone. Water Resour. Res. 57 https://doi.org/10.1029/2021wr030117.

Nogueira, G.E.H., Schmidt, C., Partington, D., Brunner, P., Fleckenstein, J.H., 2022. Spatiotemporal variations in water sources and mixing spots in a riparian zone. Hydrol. Earth Syst. Sci. 26, 1883–1905. https://doi.org/10.5194/hess-26-1883-2022.

Okruszko, T., Chormanski, J., Mirosław-Świątek, D., Gregorczyk, M., 2010. Hydrological characteristics of swamp communities, the biebrza river (NE Poland) case study. Environmental Hydraulics Taylor & Francis Group, London, pp. 407–412.

Oświt, J., 1968. Zonal arrangement of plant communities a reproduction of water conditions in the lower Biebrza river valley. Zeszyty Problemowe Postepow Nauk Rolniczych 83, 217–232. In Polish.

Pałczyński, A., 1984. Natural differentiation of plant communities in relation to hydrological conditions of the Biebrza valley. Polish Ecological Studies 10, 347–385.

Park, E., Latrubesse, E.M., 2015. Surface water types and sediment distribution patterns at the confluence of mega rivers: The Solimoes-Amazon and Negro Rivers junction. Water Resour. Res. 51, 6197–6213.

Partington, D., Brunner, P., Simmons, C., Therrien, R., Werner, A., Dandy, G., Maier, H., 2011. A hydraulic mixing-cell method to quantify the groundwater component of streamflow within spatially distributed fully integrated surface water-groundwater flow models. Environ. Model. Softw. 26, 886–898. https://doi.org/10.1016/j.envsoft.2011.02.007.

Partington, D., Brunner, P., Frei, S., Simmons, C.T., Werner, A.D., Therrien, R., Maier, H. R., Dandy, G.C., Fleckenstein, J.H., 2013. Interpreting streamflow generation mechanisms from integrated surface-subsurface flow models of a riparian wetland and catchment. Water Resour. Res. 49, 5501–5519. https://doi.org/10.1002/wrcr.20405.

Peng, H., Xia, H., Shi, Q., Chen, H., Chu, N., Liang, J., Gao, Z., 2022. Monitoring spatial and temporal dynamics of wetland vegetation and their response to hydrological conditions in a large seasonal lake with time series Landsat data. Ecol. Ind. 142, 109283 https://doi.org/10.1016/j.ecolind.2022.109283.

Peters, J., Baets, B.D., Verhoest, N.E., Samson, R., Degroeve, S., Becker, P.D., Huybrechts, W., 2007. Random forests as a tool for ecohydrological distribution modelling. Ecol. Model. 207, 304–318. https://doi.org/10.1016/j.ecolmodel.2007.05.011.

Sebben, M.L., Werner, A.D., Liggett, J.E., Partington, D., Simmons, C.T., 2013. On the testing of fully integrated surface-subsurface hydrological models. Hydrol. Process. 27 (8), 1276–1285.

Silvertown, J., Dodd, M.E., Gowing, D.J.G., Mountford, J.O., 1999. Hydrologically defined niches reveal a basis for species richness in plant communities. Nature 400, 61–63.

Slivinski, L.C., Compo, G.P., Whitaker, J.S., Sardeshmukh, P.D., Giese, B.S., McColl, C., Allan, R., Yin, X., Vose, R., Titchner, H., Kennedy, J., Spencer, L.J., Ashcroft, L., Bronnimann, S., Brunet, M., Camuffo, D., Cornes, R., Cram, T.A., Crouthamel, R., DomAnguez-Castro, F., Freeman, J.E., Gergis, J., Hawkins, E., Jones, P.D., Jourdain, S., Kaplan, A., Kubota, H., Blancq, F.L., Lee, T.C., Lorrey, A., Luterbacher, J., Maugeri, M., Mock, C.J., Moore, G.K., Przybylak, R., Pudmenzky, C., Reason, C., Slonosky, V.C., Smith, C.A., Tinz, B., Trewin, B., Valente, M.A., Wang, X. L., Wilkinson, C., Wood, K., Wysyński, P., 2019. Towards a more reliable historical reanalysis: Improvements for version 3 of the Twentieth Century Reanalysis system. Q. J. R. Meteorol. Soc. 145, 2876–2908. https://doi.org/10.1002/qj.3598.

Statistics Poland, 2021. Population by sex, feminization rate, population density. Teritorial units: Podlaskie and Warminsko-Mazurskie. as of day 31 XII 2021. accessed: 18 XII 2022. URL: swaid.stat.gov.pl. Główny Urząd Statystyczny (Statistics Poland), Warsaw, Poland.

Światek, D., Szporak, S., Chormanski, J., Okruszko, T., 2008. Hydrodynamic model of the Lower Biebrza River flow - a tool for assessing the hydrologic vulnerability of a floodplain to management practices. Ecohydrol. Hydrobiol. 8, 331–337.

Todd, M.J., Muneepeerakul, R., Pumo, D., Azaele, S., Miralles-Wilhelm, F., Rinaldo, A., Rodriguez-Iturbe, I., 2010. Hydrological drivers of wetland vegetation community distribution within everglades national park, florida. Adv. Water Resour. 33, 1279–1289. https://doi.org/10.1016/j.advwatres.2010.04.003.

Van Loon, A., Schot, P., Griffioen, J., Bierkens, M., Batelaan, O., Wassen, M., 2009. Throughflow as a determining factor for habitat contiguity in a near-natural fen. J. Hydrol. 379, 30–40. https://doi.org/10.1016/j.jhydrol.2009.09.041.

Wassen, M.J., Joosten, J.H.J., 1996. In search of a hydrological explanation for vegetation changes along a fen gradient in the Biebrza Upper Basin (Poland). Vegetatio 124, 191–209. https://doi.org/10.1007/bf00045494.

Wassen, M.J., Peeters, W.H.M., Olde Venterink, H., 2002. Patterns in vegetation, hydrology and nutrient availability in an undisturbed river floodplain in Poland. Plant Ecol. 165, 27–43. https://doi.org/10.1023/A:1021493327180.

Wassen, M.J., Okruszko, T., Kardel, I., Chormanski, J., Swiatek, D., Mioduszewski, W., Bleuten, W., Querner, E.P., El Kahloun, M., Batelaan, O., Meire, P., 2006. Eco-hydrological functioning of the biebrza wetlands: Lessons for the conservation and restoration of deteriorated wetlands rid c-7306-2008. Wetlands: Functioning. Biodivers. Conserv. Restoration 191, 285–310.

Werner, B.J., Lechtenfeld, O.J., Musolff, A., de Rooij, G.H., Yang, J., GrAffindling, R., Werban, U., Fleckenstein, J.H., 2021. Small-scale topography explains patterns and dynamics of dissolved organic carbon exports from the riparian zone of a temperate, forested catchment. Hydrol. Earth Syst. Sci. 25, 6067–6086. https://doi.org/10.5194/hess-25-6067-2021.

Yao, S., Li, X., Liu, C., Zhang, J., Li, Y., Gan, T., Liu, B., Kuang, W., 2020. New assessment indicator of habitat suitability for migratory bird in wetland based on hydrodynamic model and vegetation growth threshold. Ecol. Ind. 117, 106556 https://doi.org/10.1016/j.ecolind. 2020.106556.

Zhu, Z., Yang, Z., Huai, W., Wang, H., Li, D., Fan, Y., 2020. Growth-decay model of vegetation based on hydrodynamics and simulation on vegetation evolution in the channel. Ecol. Ind. 119, 106857 https://doi.org/10.1016/j.ecolind.2020.106857.